AR-010-463

DSTO

# Crack Growth Behaviour of Spur Gears: A Fractographic Analysis

C. Vavlitis

DSTO-TN-0137

APPROVED FOR PUBLIC RELEASE



DEPARTMENT ◆ OF DEFENCE

DEFENCE SCIENCE AND TECHNOLOGY ORGANISATION

# Crack Growth Behaviour of Spur Gears: A Fractographic Analysis

*C. Vavlitis*

**Airframes and Engines Division**
**Aeronautical and Maritime Research Laboratory**

DSTO-TN-0137

## ABSTRACT

Vibration Analysis offers a means of detecting faults in gear systems without the need for costly periodic overhaul and inspection, and promises substantial cost savings in several military platform applications. The correlation of vibration analyses with fatigue crack growth forms an essential part of ongoing research aimed at maximising the information which can be obtained from vibration analyses. This report discusses the use of fractographic analysis to determine the growth behaviour of fatigue cracks in four case-hardened low-alloy steel spur gears.



**RELEASE LIMITATION**

*Approved for public release*

DEPARTMENT OF DEFENCE

DEFENCE SCIENCE AND TECHNOLOGY ORGANISATION

*Published by*

*DSTO Aeronautical and Maritime Research Laboratory*
*PO Box 4331*
*Melbourne Victoria 3001 Australia*

*Telephone: (03) 9626 7000*
*Fax: (03) 9626 7999*

*AR-010-463*
*January 1998*

**APPROVED FOR PUBLIC RELEASE**

# Crack Growth Behaviour of Spur Gears: A Fractographic Analysis

## Executive Summary

AMRL have developed techniques for early detection and diagnosis of machinery faults using vibration analysis. These techniques offer the potential for replacing or minimising costly periodic gearbox overhauls and inspections. A major requirement, however, is validation of the vibration analysis methods using information derived from alternative defect analyses. A dynamic test rig has been set up to generate fatigue cracks in four 'aircraft quality' spur gears. This aims to establish a correlation between fault indices generated from in-house vibration monitoring software, and the actual fault growth. The fault index used is the kurtosis which is an indication of the localised damage of the gear tooth. While surface inspections provide some indication of crack growth, detailed investigation of the growth into the gear is required, to correlate crack size with the fault index.

Quantitative fractography techniques have been used by AMRL for over 20 years. These techniques are still being refined and new methods are being developed. Such analyses can be used to diagnose failures and to obtain both qualitative and quantitative information. The fractographic analysis of a fatigue fracture involves understanding that specific marks on the fracture are the result of specific events in the load history which produced the cracking. Consequently a crack depth versus time curve can be produced which ideally will represent the crack growth from an initial defect up to the crack depth at which the component failed or the crack was opened.

This report documents the detailed investigation of the fracture surfaces of the gears to determine their crack growth curves. Many factors contributed to the difficulty of locating marks, such as three dimensional relief and the fragmented nature of the crack front. While the gears showed the expected trend of crack depth increasing with time, some showed an initial rapid crack propagation followed by a slower propagation rate. This was due primarily to the significant change in loading applied to the gears. Correlations were made with the kurtosis trend and the surface inspection results, which have been found to be useful in gear rig tests as an indication of the presence and approximate location of the crack respectively. Recommendations were suggested to modify the operation of the gear rig to produce more useful crack growth curves.

This analysis will assist in developing crack growth data from vibration analysis data, and will therefore help to provide vibration analysis results which can be related to gear life in service.

# Contents

# 1. Introduction

## 1.1 Background

Four pairs of case-hardened low-alloy steel spur gears were tested as part of ongoing research at AMRL into fault detection using vibration analysis. Such analysis can provide warning of the development of cracks and other faults in gear systems, and a major research objective is therefore to establish a correlation between the actual fault growth and the condition indices generated using the vibration techniques. Currently, the progress of the crack is physically monitored by a non-destructive inspection technique called the Magnetic Rubber Inspection (MRI) technique, which has significant limitations.

Fractographic techniques were used to determine the crack growth curves for these gears. These results have been correlated with the MRI results and finally with one of the condition indices.

## 1.2 Fractography

Fractography is the analysis of fracture surfaces. Fractographic assessment of fatigue cracking has been used for many years to diagnose failures and to obtain both qualitative and quantitative information about crack growth. The diagnosis of fatigue usually includes a detailed and careful examination and analysis of the markings which are present on the fracture surface. The spacing and occurrence of these marks can be used as a quantitative assessment of crack propagation rate and cyclic history. Both optical and electron microscopes are used to observe the fractures. The quality, direction and nature of the lighting employed for the examination is a crucial factor in the microscopic examination of fractures. This will become apparent in subsequent sections of this report, which details the fractographic analysis of the four gears.

# 2. Fractographic Methods

A large amount of information can be obtained about crack growth using fractographic methods. The actual fracture mode can be established, initiation sites can be located, and if the load history is known, it is usually possible to obtain a crack growth curve for a fatigue fracture, relating crack size and events in the load history.

A fracture can be examined in two ways - macroscopically and microscopically.

## 2.1 Macroscopic Examination

Typically, macroscopic examination means observation of the specimen with the unaided eye. However, in terms of fractography, it can be used to describe specimen examination up to a magnification of 50. Information can be extracted from macroscopic marks sometimes known as progression markings (see Figure 2.1). The individual marks represent successive positions of the crack front where propagation conditions change as the crack grows through the metal. They can be produced by :

(a) Variation in cyclic loads.

(b) Arrest of crack growth by a period of rest with a subsequent accretion of corrosion products at the crack tip [1].

(c) Changes in propagation mode.

*Figure 2.1 Prominent progression marks emanating from a Macchi wing spar/undercarriage attachment bolt hole*

## 2.2 Microscopic Examination

Fatigue fractures consist of 3 zones [2] which are commonly called :

| | |
|---|---|
| Stage I | Initiation zone |
| Stage II | Zone of stable crack growth |
| Stage III | Zone of accelerated crack growth. |

Cycle by cycle crack growth properties are obtained from Stage II which is characterised by the microscopic marks known as striations shown in Figure 2.2. Each striation is a representation of the advance of the crack in one load cycle, and counting can be used to analyse the crack propagation portion of fatigue life. Striations are more readily visible in ductile materials which have many active slip planes, and are less visible in high strength steel which has a smaller number of active slip planes than aluminium alloy.

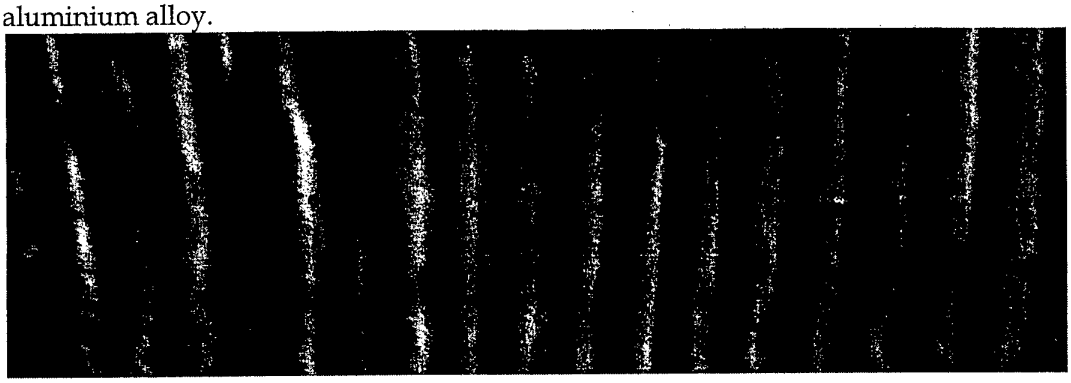

*Figure 2.2 Fatigue striations in a 7050 aluminium alloy, compact tension specimen, 5000x*

# 3. Gear Rig Tests

This investigation originated in another task conducted at AMRL, investigating faults in spur gears [3].

A spur gear rig has been set up whereby a pair of case-hardened low-alloy steel, spur gears are run under load. The gears have a spark-eroded notch initiated at the root of the tooth of the pinion gear, to provide a definite initiation site for a crack and to guarantee the growth of a crack. The purpose is to establish a correlation between the mechanical condition of the gear, ie the crack growth, and the fault indices generated from vibration analysis techniques.

One of these indices is the kurtosis (the fourth statistical moment). This is an indication of the peakiness of the signal corresponding to a localised fault, which in this case is the crack in the tooth. Experience suggests values of kurtosis over 3.5 are regarded as indicating the presence of a crack.

A non-destructive inspection technique used to monitor the crack growth after each run of the rig is the Magnetic Rubber Inspection (MRI) technique. This method is based on magnetising the specimen, and applying a rubber solution which contains magnetic particles to the suspect area. The particles become aligned around the crack due to a disruption in the magnetic field, highlighting the crack path which can then be measured by a calibrated microscope.

This method provides a good estimate of the propagation of the crack on the surface but gives no indication of the crack depth. For that reason, fractographic techniques are required to derive a reliable crack growth rate. The four gears used in the recent tests were labelled A2-1, A2-2, A2-3 and A2-5. A2-4 was not used since it was discovered that the crack did not run parallel with the root of the tooth. All gears were identical in terms of their material, heat treatment and notch geometry. Each gear had a crack-starting notch size of 2mm long, 0.1mm wide and 1.0mm radius deep.

# 4. Loading On Gears

Figures 4.1 to 4.4 show the loading sequences applied to the gears. The loading was dependent on the kurtosis level. To prevent damage to the gears, as soon as the kurtosis exceeded a given critical value, the load was reduced. Similarly, if there was no change in the kurtosis for a long period of time, the load would be incremented.

## 4.1 Loading of Gear A2-1

The loading sequence for this gear consisted of four runs as can be seen in Figure 4.1. The rig was run at the maximum load of 45kW for the entire first run. After approximately 3.5 hours the monitoring system showed the kurtosis to increase to a value of 3.25, at which point the rig was shut down. In the second run, the kurtosis jumped quite significantly when the load reached 39kW. Hence when it was further increased to 45kW the increase of kurtosis to approximately 4.2 resulted in an immediate unloading sequence and end of the run. Lower loads were applied in the third run to produce a more gradual propagation of the crack and to minimise any discrepancies between the kurtosis indices and the actual condition of the cracked tooth. Hence the load was left at 33kW and after 45 minutes the unloading sequence began. In the final run, the load was started at a conservative level of 5kW since the crack had already progressed by an extensive amount (as indicated by the MRI results, see Section 6). The rig was shut down at a loading of 10kW.

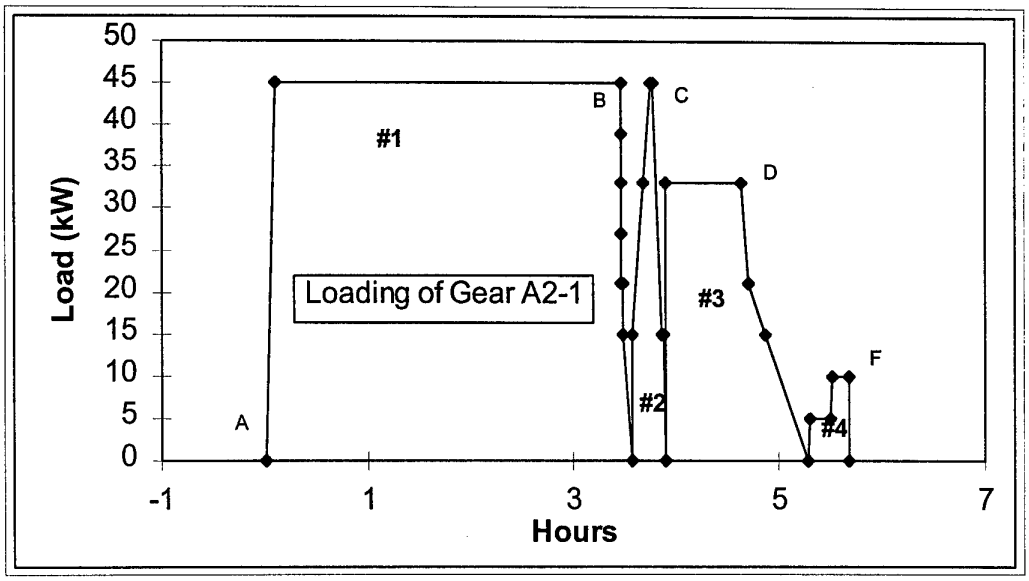


*Figure 4.1 Loading sequence of Gear A2-1*

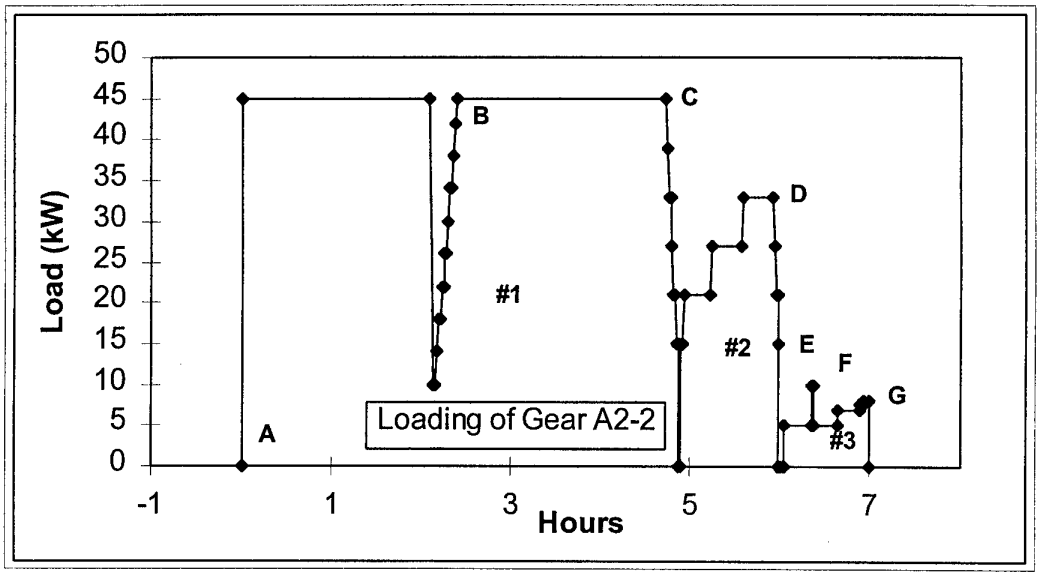


*Figure 4.2 Loading sequence of Gear A2-2*

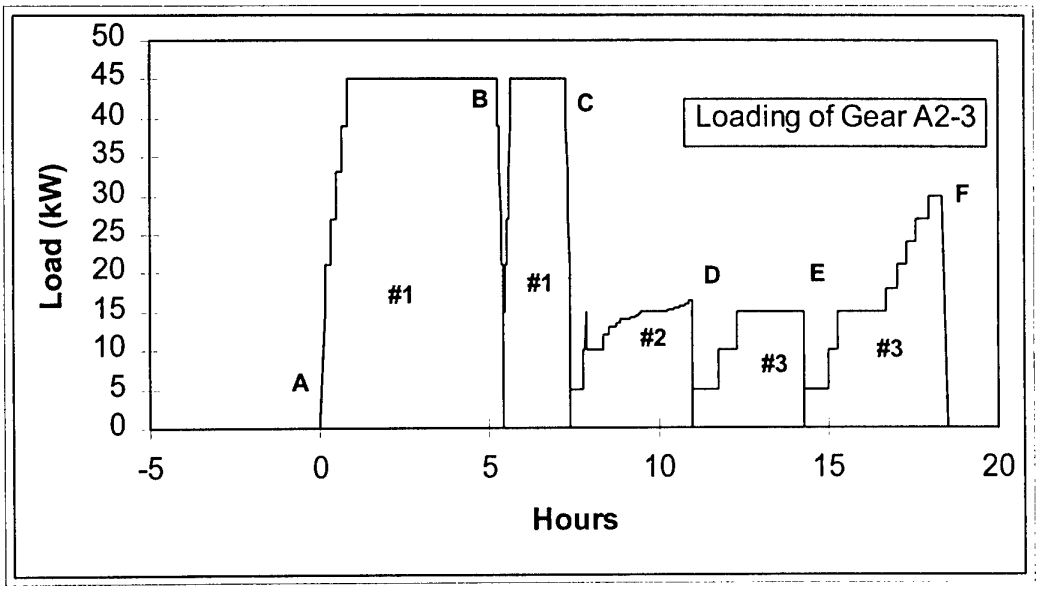


*Figure 4.3 Loading sequence of Gear A2-3*

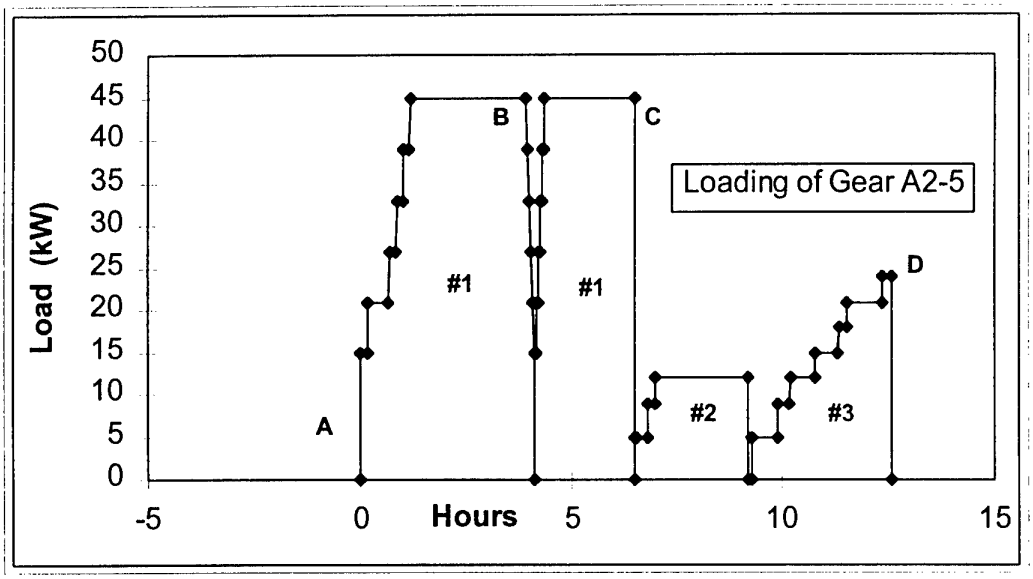


*Figure 4.4 Loading sequence of Gear A2-5*

## 4.2 Loading of Gear A2-2

The loading sequence for this gear consisted of three runs as can be seen in Figure 4.2. In the first run the gears were loaded at the full load of 45kW as for the previous gear. Only this time, at approximately two hours into the run, the load was reduced to 10kW and then reloaded to 45kW. This was done for reference purposes. The second run had the gears loaded to 21kW initially whilst the kurtosis was being monitored. Loading was then increased to 27kW and then to 33kW, where after a while the kurtosis began to rise steadily. Once the kurtosis reached a critical value the rig was shut down. The final run started with a conservative load again of 5kW. When this was increased to 10kW there was a sudden increase in kurtosis and the load was reduced immediately. Then as can be seen, the load was increased in small steps until the kurtosis value indicated a substantial amount of crack propagation.

## 4.3 Loading of Gear A2-3

The loading sequence for Gear A2-3 consisted of three runs, with the first and third run split over two days, as indicated in Figure 4.3. A load of 45kW was maintained throughout the first run, however it should be noted that approximately 2 hours into the run there was a sharp drop in the kurtosis which can not be noticed in Figure 4.3. The second day of the first run was also maintained at 45kW until such time that the kurtosis signified a crack in the tooth. The second run started at a conservative level of 5kW. A sharp peak is seen at the point where the load was increased to 15kW resulting in a sudden kurtosis jump. The load was then increased in stages once the kurtosis increase was stabilised. This continued until shut down at 16.3kW. The third run began at a loading of 5kW and then to 10kW once the kurtosis had time to settle. It was at 15kW that the kurtosis increased and the rig shut down at the end of the working day. In the final day, the loading was left at 15kW for the bulk of the time, to give the kurtosis time to gradually increase. Towards the end of the run, the gears were loaded up in steps, until at 30kW, the kurtosis increased steadily. This indicated the crack was propagating and the rig was shut down.

## 4.4 Loading of Gear A2-5

The loading sequence for Gear A2-5 also consisted of three runs with the first run split over two days, as indicated in Figure 4.4. The loading was similar to the earlier sequence of Gear A2-3. The gears were loaded at 45kW for the first and second day of the first run. The rig was shut down when the kurtosis climbed to a value of 3.7 at approximately 6.5 hours. In the second run, there was a sustained rise in the kurtosis at the load level of 12kW. The run was terminated at approximately 9 hours. The final run consisted of varying load increases with an accompanying fluctuation in the kurtosis trend, but there was nothing to indicate the progression of the crack. Hence the run was completed at approximately 12 hours.

# 5. Surface Photographs

Before the fracture surfaces of the gears were investigated, digital photographs were taken of the surface of the gears. To obtain a simple photograph, the lighting had to be manipulated extensively to get illumination which would show the crack. The problem was that each gear had grinding marks produced from manufacture, and these marks sometimes ran in the same direction as the crack, making the crack very difficult to see. The photographs were captured digitally using Adobe Photoshop. Figure 5.1 is a surface image acquired of Gear A2-3, showing the crack from the root of the tooth extending into the middle of the tooth.

The images were calibrated and the final crack length was measured using a line measuring tool. This was done in two ways. First a simple straight line estimate was obtained from the root of the notch where the edge crack started, (indicated by the white arrow in Figure 5.1), to the end of the crack. Secondly the distance was measured by tracing out a line along the crack. Although this latter measurement is a more accurate representation of the crack depth, the straight line distance was used to compare with the MRI results (see Section 6). Table 5.1 shows the distances obtained using this method on three of the four gears. Gear A2-1 had already been cut open and hence no surface photograph could be obtained. In addition the crack on the 'inside' of Gear A2-2 could not be detected due to the interference with the grinding marks. (The terms 'inside', and 'outside' when referring to the gears means the sides of the gear closest to, and farthest from, respectively, the input shaft support bearing on the gear rig).

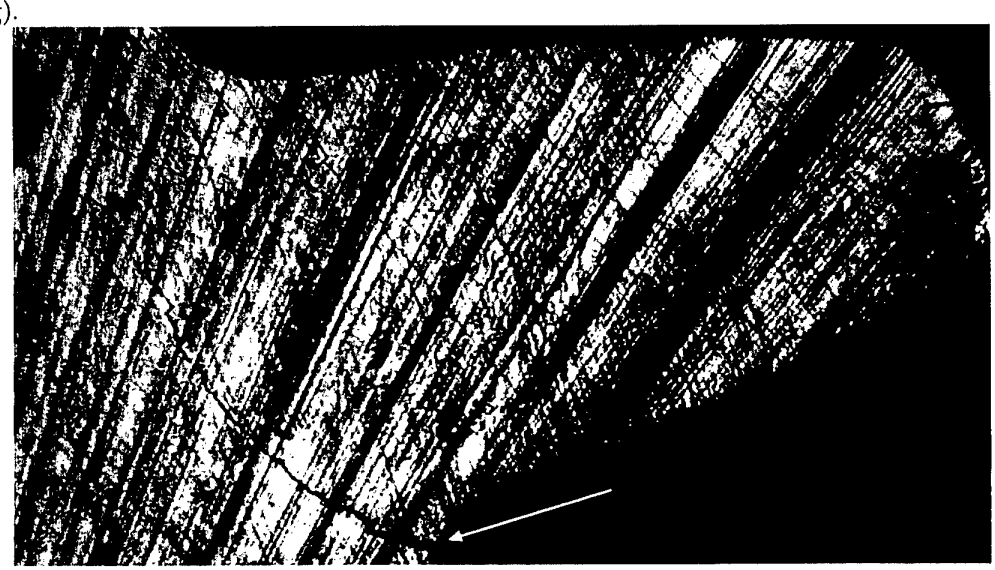

*Figure 5.1 Surface of Gear A2-3 showing edge crack (indicated by arrow)*

*Table 5.1 Surface crack depths of the gears*

| | CRACK DEPTH ( mm) | |
|---|---|---|
| GEAR | ESTIMATE | ACTUAL |
| A2-2 inside | Could not detect the crack | |
| A2-2 outside | 1.52 | 1.65 |
| A2-3 inside | 3.25 | 3.62 |
| A2-3 outside | 3.14 | 3.36 |
| A2-5 inside | 2.02 | 2.10 |
| A2-5 outside | 0.64 | 0.69 |

# 6. Magnetic Rubber Inspection (MRI)

As was stated in Section 2, the MRI technique was the non-destructive tool used to obtain the length or depth of the crack after each run of the rig. It is important to distinguish between crack length and crack depth when discussing crack measurements. The crack emanating from the notch is three dimensional. Looking at the view of the notch in the root of the tooth from the gear face (Figure 6.1), the crack can be seen extending from both sides. That length is known as the crack length. However the same crack is also penetrating into the gear, to a distance which can only be estimated visually once the crack reaches the edge of the root, as shown in Figure 6.2. This length is known as the crack depth. Hence from the MRI measurements, only the crack lengths can be measured until such time that the crack becomes an edge crack, and then the crack depths are measured.

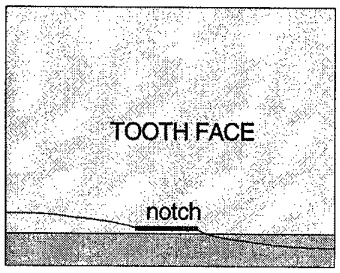


*Figure 6.1 Crack length extending from notch*

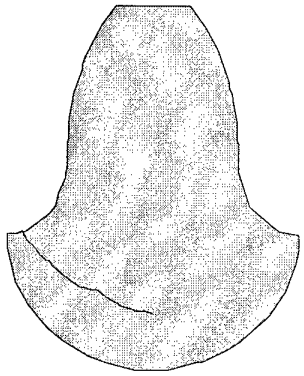

*Figure 6.2 Crack depth extending from root of tooth*

Using a microscope, the cracks were measured on all the MRI impressions. When performing MRI-measurements, it was sometimes very difficult to determine when the particles ceased to trace out a crack length. Interpretation of where the crack begins or ends is highly subjective. The results are shown in Table 6.1. Once the crack reached the edge of the tooth, its size on the inside or outside face was measured from the edge, labelled as 'down' in the table.

*Table 6.1 Crack lengths and depths obtained from Magnetic Rubber Inspection*

| | | Crack Measurements from Magnetic Rubber Impressions (mm) | |
|---|---|---|---|
| GEAR | RUN | INSIDE | OUTSIDE |
| A2-1 | 1 | 1.1 | 0.95 |
| | 2 | 1.15 | 1.05 |
| | 3 | 1.3 down | 0.55 down |
| | 4 | 2.9 down | 0.7 down |
| A2-2 | 1 | 1.5 | 1.8 |
| | 2 | 0.6 down | 1.9 down |
| | 3 | 0.7 down | 2.2 down |
| A2-3 | 1/2 | 3.2 down | can not detect |
| | 3 | 3.5 down | 3.6 down |
| A2-5 | 1 | 2.5 down | 0.85 down |
| | 3 | 2.7 down | 0.95 down |

The only values that could be compared, were the final crack depths measured from the MRI results, and the depths obtained from the surface pictures. When the MRI impressions were measured, a cross hair in the microscope eye piece was used to trace along the crack. Since this can only trace out a straight line distance, it seemed feasible to compare these values with the straight line distance taken from the surface pictures. Considering the room for error in the MRI results, the final crack depths of all the gears using both methods are in reasonable agreement. Table 6.2 shows these results.

*Table 6.2 Comparison of final crack depths*

| GEAR | Magnetic Rubber Inspection | Surface Image Estimate |
|---|---|---|
| Gear A2-2 outside | 2.2 | 1.52 |
| Gear A2-3 inside | 3.5 | 3.25 |
| Gear A2-3 outside | 3.6 | 3.14 |
| Gear A2-5 inside | 2.7 | 2.02 |
| Gear A2-5 outside | 0.95 | 0.64 |

# 7. Cutting of Gears

This part of the task was significant in that the way the gear was cut had a bearing on the results obtained. Initially a large abrasive saw was used to cut off the section surrounding the tooth of interest and including up to two adjacent teeth on both sides. Then a slow speed diamond saw was used to cut through the gears.

Precautions had to be taken to ensure that the fracture was not damaged. The gear had to be cut in such a way so that the crack could be opened easily to reveal the fracture. Clearly, it was extremely important that all the fracture was left, that is, the end of the fracture surface was not destroyed.

The distance between the end of the cut and the end of the crack needed to be smaller than the distance between the end of the cut and the surface edge of the gear, to decrease the chance of the gear being broken in the wrong place.

# 8. Fracture Surfaces

## 8.1 Optical Examination

The next stage of the investigation was to examine the fracture surfaces of all the gears, both macroscopically and microscopically, using various microscopic techniques.

### 8.1.1 Macroscopic Examination

Macroscopic examination of the fracture in a binocular microscope, provided a clear picture of the characteristics of the fracture. The first feature which was quite distinct and common to all the fractures was the extent of relief. That is the fracture was very three dimensional, and a two dimensional view could highlight different features depending on the illumination.

Typically, two main regions could be distinguished: the region of fatigue and the region of overload or fast fracture. Depending on how the gears were cut, the region of overload could usually be distinguished by its distinct change in texture and brightness. Around the notch of some of the gears, there was evidence of rubbing shown by the highly reflective smooth surface. Progression marks were obvious on some of the fractures, while on some not even one mark could be located. Some of the gears were stained; the staining was possibly caused by water or magnetic rubber being trapped in the crack.

### 8.1.2 Microscopic Examination

Steels have very different fracture characteristics from aluminium alloys. On a microscopic level, striations can be clearly observed in ductile materials such as aluminium alloys (as shown in Figure 2.2). However steels tend to produce striations which are very difficult to see. Hence, it was not surprising that the gear fractures produced few, scarce striations which only formed in discrete areas. The scanning electron microscope was used to search the fractures for striations, however even at very high magnifications, striations could only be found at a few locations around the crack front. Figure 8.1 shows a region of the fracture Gear A2-1 in which a small patch of striations are visible. (the white arrow points in the direction of crack growth).

Various techniques exist to obtain crack growth data from fracture surface markings [4]. The basic approach is to obtain calibrated images of striations at many positions along the depth of the crack. Computer-Automated techniques which can be carried out are 1D Fast Fourier Transforms, 2D Fast Hartley Transforms and Peak Count Measurements.

These techniques have all been used successfully to determine striation spacing for aluminium alloys. However, striations are usually easily seen in ductile materials. In the fractures of the steel gears, because of the difficulty of obtaining good striations at a range of crack depths, the fractography measurement was performed using the macroscopic progression marks. Such marks usually represent a significant change in loading as in the case of some of the loading sequences in the gear rig. Hence information was gathered by correlating the marks on the fracture surface with the known load sequence that was applied to the specimen.

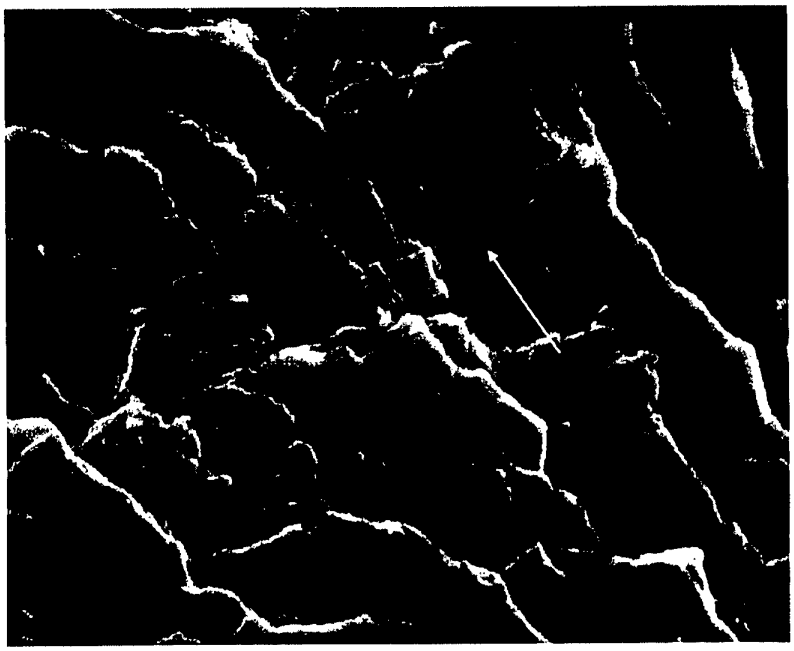

*Figure 8.1 Scanning electron micrograph of Gear A2-1 showing fragmented striations (white arrow) 5000x*

## 8.2 Digital Images of Fracture Surfaces

It was necessary to determine the best method of observing the macroscopic marks on the fracture surfaces. Surface images were acquired both digitally and with film. The film produced clear images which is essential in locating marks, and assists in the correlation with the loading. However, despite the quality of these images, the process was very time consuming. Adjustments had to be made to the focus, the lighting, the exposure, and the depth of field, to obtain one image. This did not guarantee that the resulting photo would show the desired marks.

With a digital image, all the work was done directly on the screen. The light and contrast could be adjusted on the screen until the mark required was observed. Then when all the parameters were set, the image was captured. The images could be calibrated quite easily so that distances between marks could be measured. The lines on the gears were very difficult to see and in many instances, the speed of the digital approach minimised the chance of 'losing' the location of a particular mark. (The chances of this were greater in an image taken with film since the waiting time included the developing and processing of the film). Digital imaging of the fracture surface turned out to be quicker and more effective, especially in the case of the gears.

## 8.3 Fracture Surface of the Gears

Figures 8.2 to 8.5 show the fracture surfaces of the four gears acquired using an image analysis package. Indicated also are the results of the MRI which will be discussed briefly in Section 9. These images show the overall fracture of the gears in one view. In order to see all the marks associated with the crack growth curve, the magnification had to be increased, and the lighting conditions and contrast had to be changed constantly to see the marks.

Staining can be seen clearly in Gear A2-3 and Gear A2-5. This made it even harder to see any prominent marks on the fracture. A similar problem occurred with the rubbing around the notch which can clearly be seen as the bright reflected regions in Gear A2-1 and Gear A2-5. Along the sides of most of the fractures there were some very bright regions. These actually correspond to the iron carbide particles formed during the carburising of the gears. There were more distinguishable features on these fracture surfaces. Section 10 will deal with the marks observed in detail.

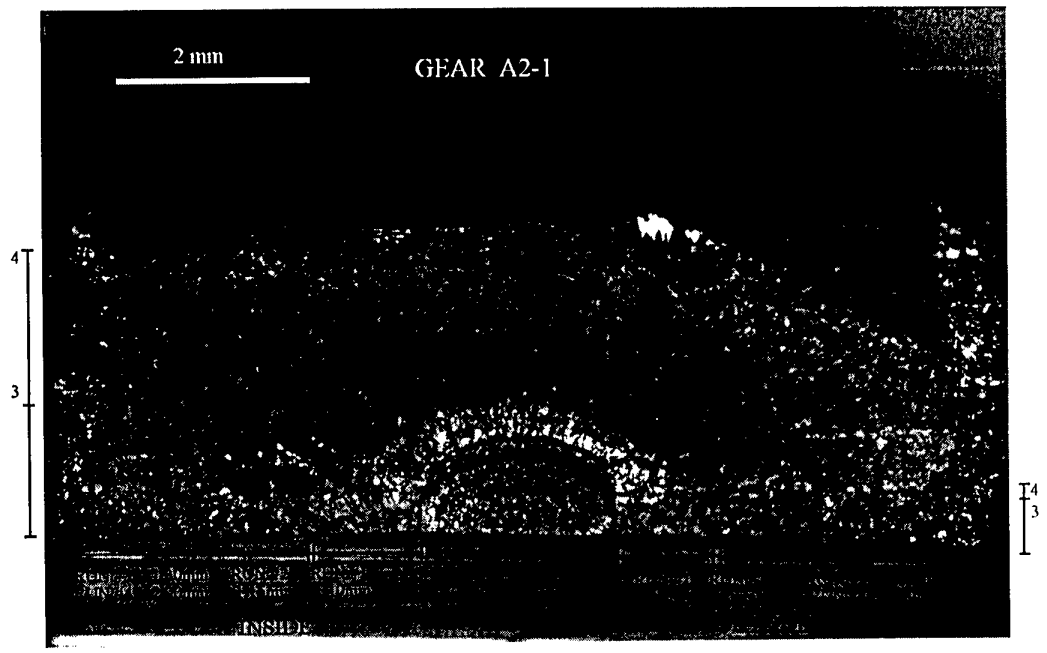


*Figure 8.2 Fracture surface of Gear A2-1 with corresponding results of the Magnetic Rubber Inspection*

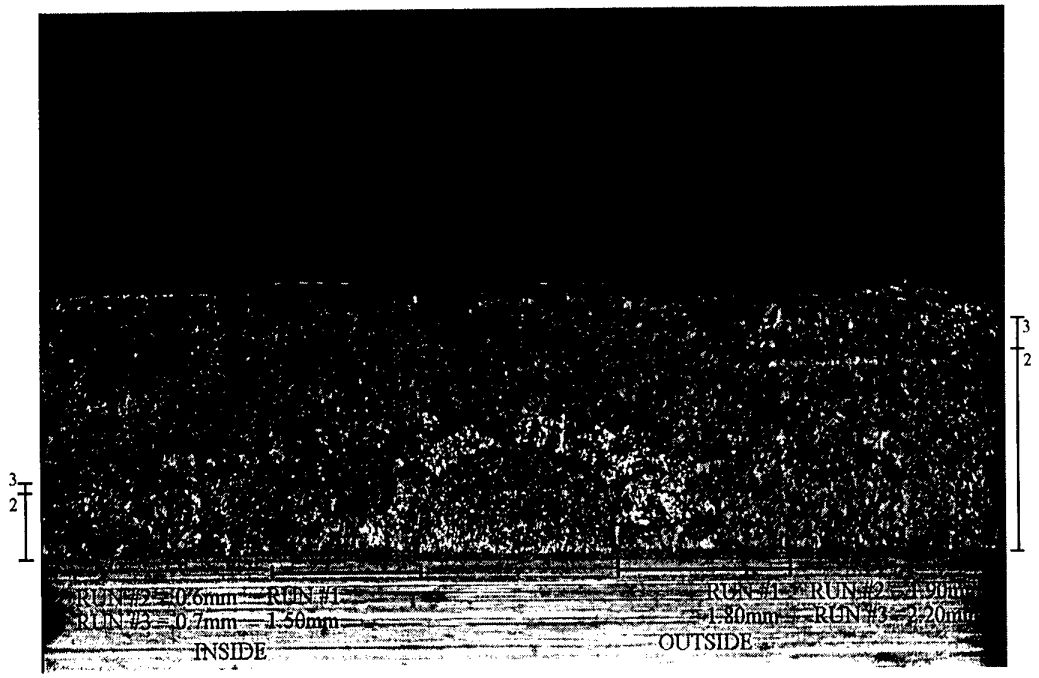


*Figure 8.3 Fracture surface of Gear A2-2 with corresponding results of the Magnetic Rubber Inspection*

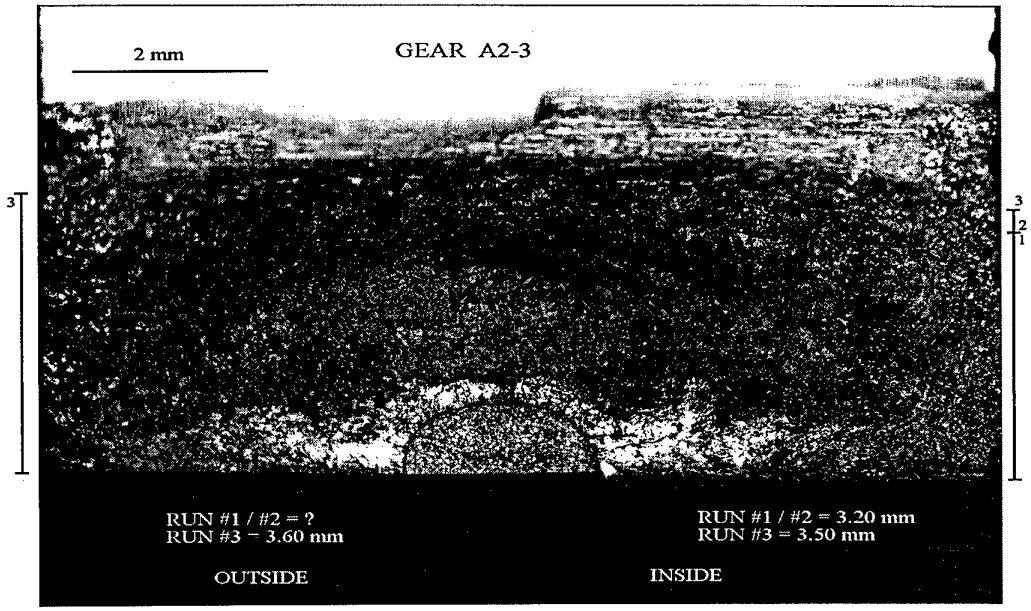


*Figure 8.4 Fracture surface of Gear A2-3 with corresponding results of the Magnetic Rubber Inspection*

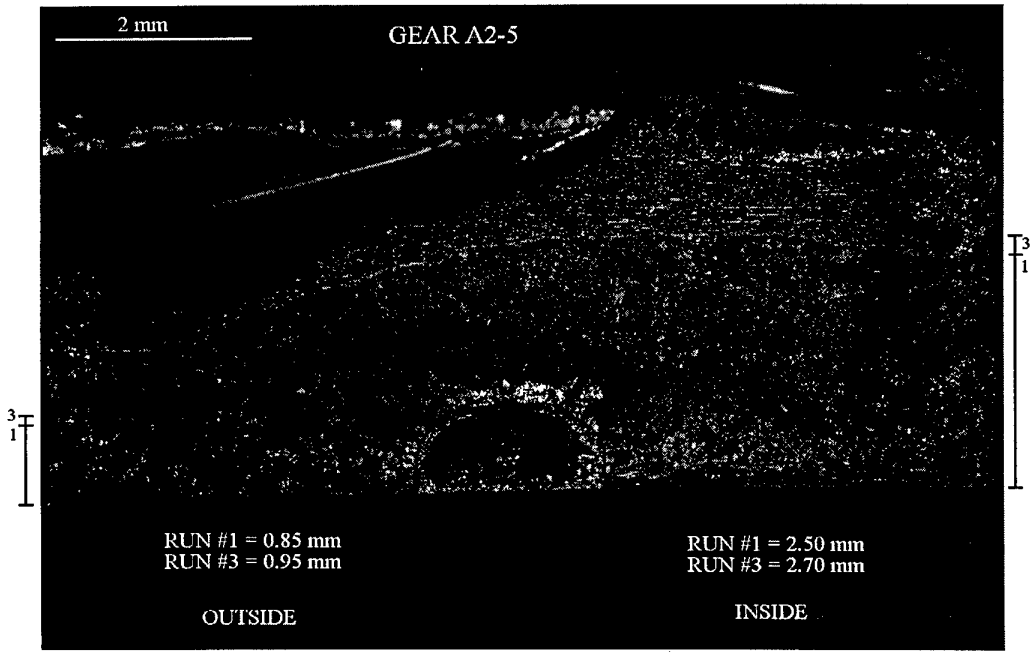


*Figure 8.5 Fracture surface of Gear A2-5 with corresponding results of the Magnetic Rubber Inspection*

# 9. Correlation with MRI Results

The MRI results obtained previously were drawn to scale over the digital images just obtained (see Figures 8.2 to 8.5). This way, the crack lengths and depths measured at the end of each run, or whenever an impression was taken, could be used as an approximate guide as to where any macroscopic progression marks should be located. When obtaining the crack growth curves, the MRI results were used as an indication of where the crack was at any stage to help with the classification of the marks.

The values of the final crack depth are compared in Table 6.2, where the MRI results are compared to the surface image depths; the values agreed reasonably well. In the fractures of Section 8, a comparison was made of the final crack depths shown on the fracture surfaces with those indicated by the MRI results. In all gears there was a good correlation. The MRI results slightly overestimate the depth as can be seen in Gear A2-5 (Figure 8.5) where the MRI estimate of the end of the third run, is beyond the line where it fractures. The MRI results also overestimated the crack size in Table 6.2.

# 10. Crack Growth Curves

Many different images were used to determine which marks on the fracture correlated with loads from the sequence. The marks were dependent on which microscope was used, and extremely dependent on the quality of illumination. The procedure for obtaining the crack growth curves for all four gears was as follows.

Once a mark was observed, the load history curves (Figures 4.1 to 4.4) were used to determine which load feature caused that particular mark. Since progression marks arise due to arrests of the crack by periods of rest or by variation in cyclic loads, the end of a run should produce a mark, since the load drop is significant. Also any other time when the load was suddenly increased or decreased during the run should result in a mark. The term load feature is used to describe these instances. This was repeated for all the marks until a final correlation was obtained for the marks and their corresponding load features.

The distance to that mark was measured from the centre of the notch and the time in hours associated with that mark was noted. It was important to measure all the marks along the same line since the crack behaved differently on different sides of the notch. Then the actual crack depth measurements were obtained by calibrating the image.

Finally plots of crack depth versus time in hours were obtained in conjunction with plots of the log of the crack depth versus time. (The reason for this is because a log-linear curve of crack growth under a stable loading condition is often observed to produce a straight line).

## 10.1 GEAR A2-1

Table 10.1 indicates the distances to each mark shown with their corresponding load feature. Each record contains the load which produced it, the time of that load in hours, and a label for that mark (in this case from A to F). Also two distances are seen in the final two columns. The first is the raw depth which is simply the distance to the mark from the centre of the notch as measured from the image. The final column shows the actual distance of the crack using the scaling factor for that image. The format of this table is the same for each gear. The marks on the fracture surface of Gear A2-1 can be seen in Figure 10.1, indicated by the arrows. (Note that these marks will not always be visible in this report as they were on the screen).

The first point used on the crack growth curve was the initiation site since this is a known location on a macroscopic scale. At time = 0 hours the crack depth equals the notch radius since the distances were taken from the centre of the notch. The notch has a length of 2mm and hence the radius is approximately 1mm. This is the mark labelled A in Figure 10.1.

The aim was to match the marks seen with the most prominent part of the load history. Marks B and C were the most prominent in this fracture surface. They were seen running parallel along the right side of the notch but were not very clear on the left side. For that reason the right side of the fracture was the focus for this gear. Looking at the load history, for Gear A2-1 (Figure 4.1) the two prominent load features were obviously at the end of runs one and two. The load at this time was reduced from 45kW down to zero and with such a significant drop in load occurring within an hour from each other, it is feasible to expect two distinct marks close to each other.

The final mark (F) was known, since obviously the crack ceased growing when the last run was completed.

The final two marks were ones that were observed using different lighting conditions and higher magnification. Mark D is a mark that can be clearly seen on the boundary but not very well on the inner surface. It corresponds to the end of run number 3. Finally, mark E is a small mark corresponding to the last run when the load is incremented from 5kW to 10kW. The crack depth versus time curve resulting from this, can be seen in Figure 10.2. The general trend of crack depth increasing with time can be seen quite clearly. The corresponding log-linear curve is shown in Figure 10.3.

*Table 10.1 Crack growth analysis for Gear A2-1*

| Run | Date | Time (hours) | Load (kW) | Mark Label | Raw depth (mm) | Crack Depth (mm) |
|---|---|---|---|---|---|---|
| 1 | 4/04/96 | 0 | 0 | A | 37 | 1 |
| 1 | 4/04/96 | 3.4667 | 45 | B | 95 | 2.57 |
| 2 | 18/4/96 | 3.7536 | 45 | C | 101 | 2.73 |
| 3 | 23/4/96 | 4.6383 | 33 | D | 115 | 3.11 |
| 4 | 5/03/96 | 5.5064 | 5 | E | 141 | 3.81 |
| 4 | 5/03/96 | 5.69 | 0 | F | 154 | 4.16 |

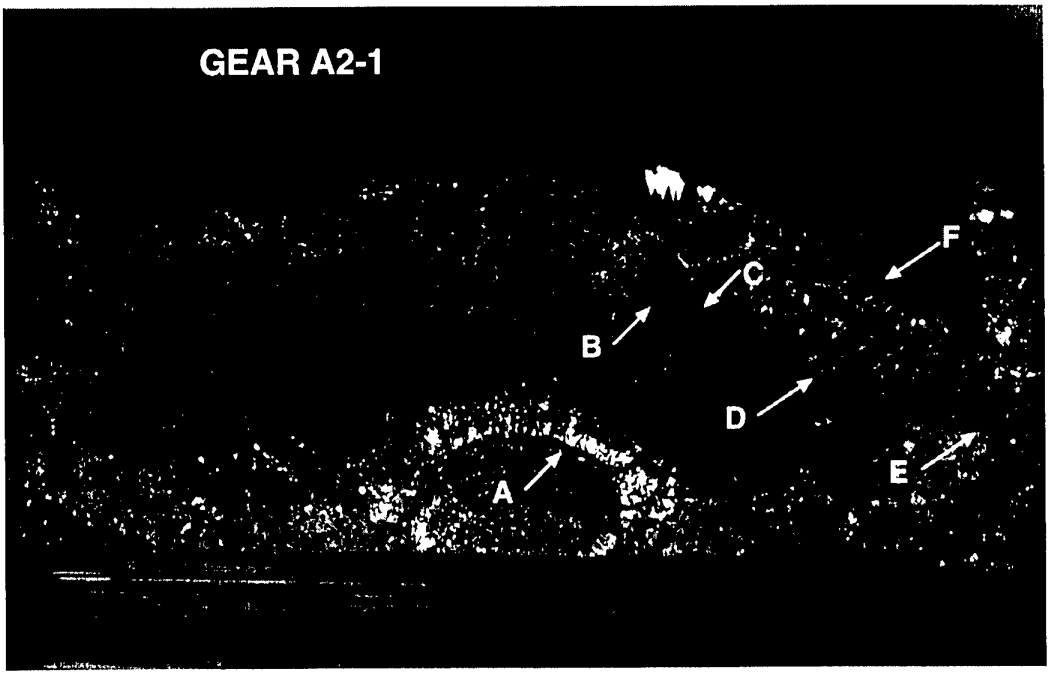


*Figure 10.1 Indication of progression marks on fracture surface of Gear A2-1*

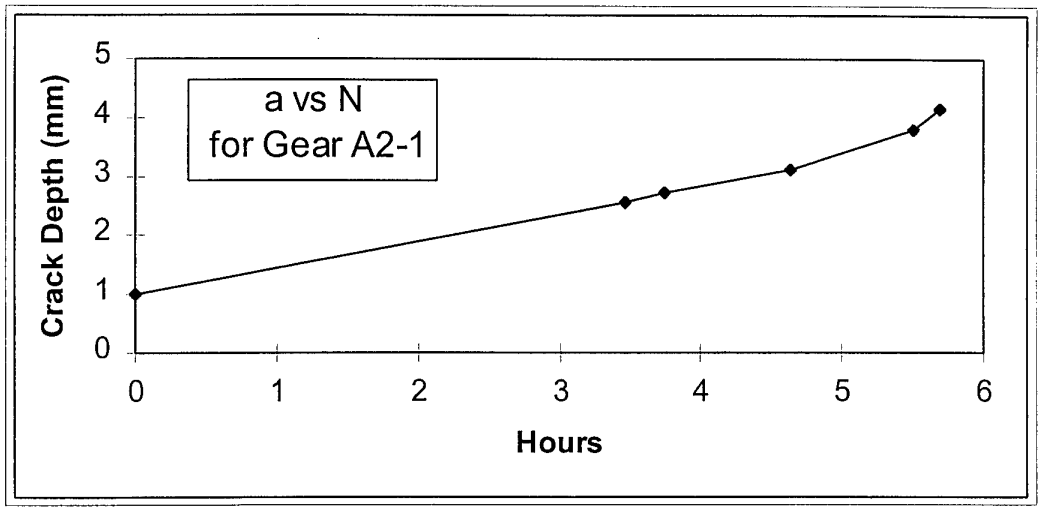


*Figure 10.2 Crack growth curve for Gear A2-1*

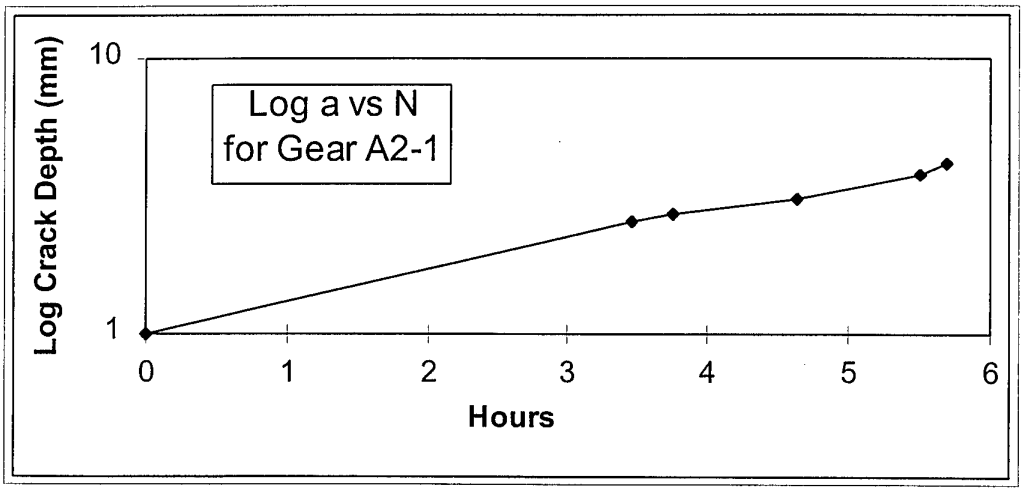


*Figure 10.3 Log-Linear crack growth curve for Gear A2-1*

## 10.2 GEAR A2-2

The next gear investigated was Gear A2-2. Table 10.2 shows the data relating to this gear, similar to Table 10.1. Figure 10.4 shows the fracture surface for Gear A2-2 with the marks indicated by the white arrows.

This fracture surface did not have any obvious distinguishing marks like Gear A2-1. The marks were all very subtle, making it extremely difficult to correlate the loads with the markings. In fact Gear A2-1 was the only gear of the four that showed the two macroscopic marks clearly.

The first mark corresponded to the known point of crack initiation. Once again at time = 0 hours, the crack depth is 1mm or equal to the notch radius. This assumed that the crack started at the end of the notch immediately. The fact that the gears failed in such a short time, the gears contained such a big initial defect and extreme loading conditions were applied to the gears, support the assumption that the crack started to progress immediately from the notch.

The second known point was the end of the crack which could usually be seen quite clearly in any fracture. However in this fracture, the fast fracture region could not be located. The explanation for this is that the cuts used to section the gear were within the fatigue fracture zone, thus preventing the full exposure of the fracture. After detailed observation, a small portion of overload fracture was noticed in the top right corner of the fracture indicating the end of the crack. This mark is labelled G as shown in Figure 10.4. Hence the area of observation was concentrated in this area where a straight line could be constructed between the notch and the end of the crack.

This fracture also exhibited two distinct marks which were very dark and noticeable once the region was magnified. Initially these marks were correlated with the two load features in the middle and end of the first run. This seemed logical since they both contained a sharp drop in load from 45kW. However on further inspection, another mark (B) was located near the notch which challenged the correlation made previously. It suggested that mark B was associated with the peak in the middle of the first run and the previous two marks (C and D) corresponded with the end of the first run and the end of the second run respectively. This was a more satisfactory interpretation, since the first peak occurred fairly early in the loading sequence implying that the mark would need to be close to the notch.

Finally the two marks E and F were subtle marks found between mark D and the end of the crack. These corresponded with the first sharp rise to 10kW and also the second rise to 7kW in the final run.

The crack growth curve can be seen in Figure 10.5. As with the curve for Gear A2-1, the trend is as expected. The log-linear curve is shown in Figure 10.6.

*Table 10.2 Crack growth analysis for Gear A2-2*

| Runs | Date | Time (hours) | Load (kW) | Mark Label | Raw depth (mm) | Crack Depth (mm) |
|---|---|---|---|---|---|---|
| 1 | 13/05/96 | 0 | 0 | A | 37 | 1 |
| 1 | 13/05/96 | 2.085 | 45 | B | 56 | 1.51 |
| 1 | 13/05/96 | 4.7333 | 45 | C | 87 | 2.35 |
| 2 | 14/05/96 | 5.9139 | 33 | D | 119 | 3.22 |
| 3 | 15/05/96 | 6.35809 | 10 | E | 144 | 3.89 |
| 3 | 15/05/96 | 6.639433 | 7 | F | 160 | 4.32 |
| 3 | 15/05/96 | 6.9958 | 0 | G | 177 | 4.78 |

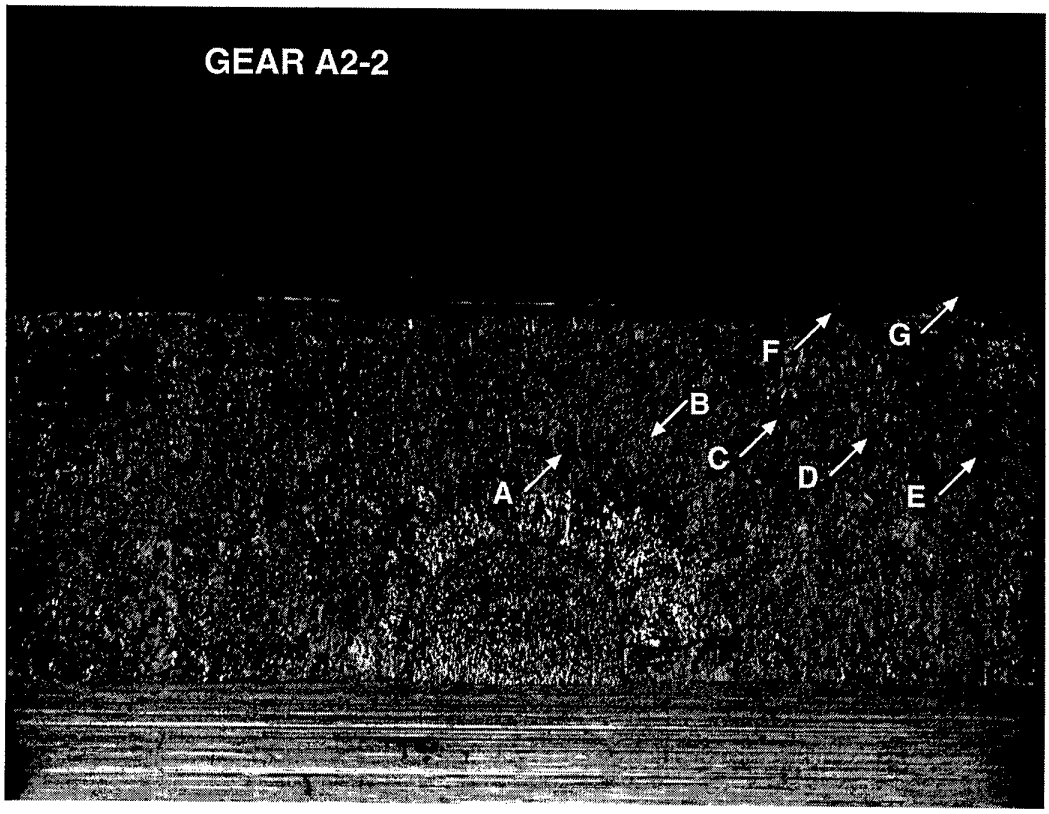


*Figure 10.4 Indication of progression marks on fracture surface of Gear A2-2*

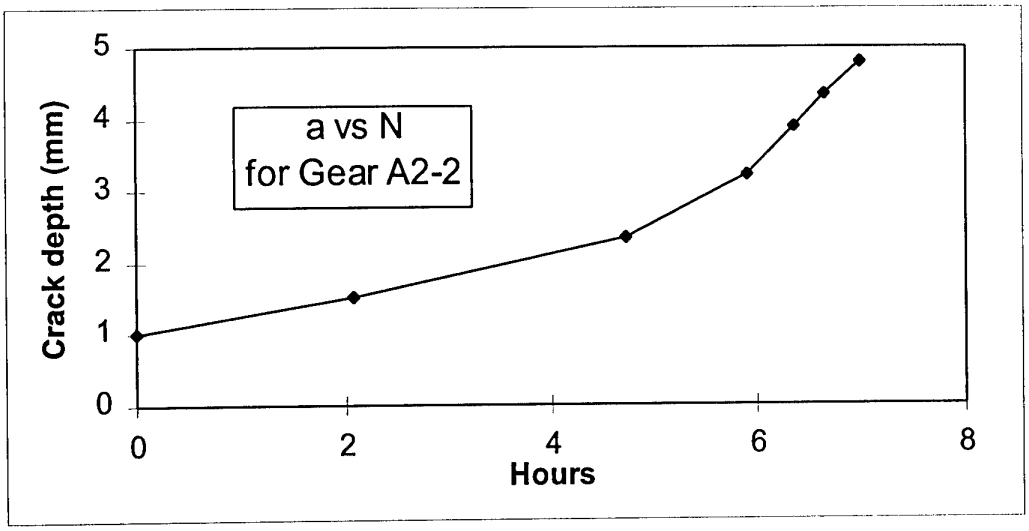


*Figure 10.5 Crack growth curve for Gear A2-2*

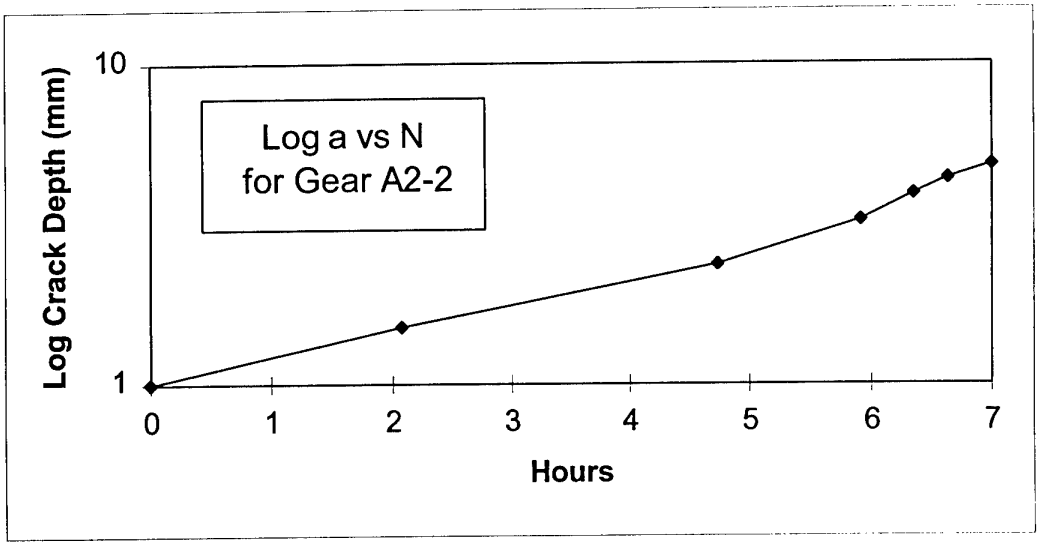


*Figure 10.6 Log-Linear crack growth curve for Gear A2-2*

## 10.3 GEAR A2-3

This was a more difficult fracture to analyse compared to the previous two gears. The fracture was very textured and markedly three dimensional. Also the stain in the middle of the specimen made it difficult to locate marks. The most prominent feature of the fracture was the region of texture change. A change like this is characteristic of a crack that has reached the edge of the gear, or possibly when the stress has changed in a significant way. In that region, both of the above had occurred. The crack had changed from a surface to an edge crack, and the loading was significantly reduced. The table of data for this gear is shown in Table 10.3 and the corresponding fracture surface showing the marks as white arrows is seen in Figure 10.7.

As with the previous gears, the first point on the crack curve coincided with the initiation site at the notch tip (mark A). The region of overload could be observed very easily (although out of focus in Figure 10.7, mark F), hence the final point was easily obtained. This gear proved to be a challenging fracture to analyse, due to a distinct mark occurring close to the notch. This will be discussed below as two separate analysis attempts.

### 10.3.1 First Attempt

The first distinct mark observed was that of mark C, which is the mark occurring straight after the texture change. It was mentioned that the texture change was possibly due to a significant load change. Hence looking at the load history, it seemed logical that this mark should correspond with the end of the first run since the loading there dropped significantly from 45kW to a maximum of 16.3kW in the second run.

However on observing the fracture there were two distinct marks between the notch and mark C. Mark N was a very definite mark which could be traced along the whole crack front. This meant that mark C could not be correlated with the end of run one since there were two distinct markings before it but only one load drop. Therefore mark N had to correspond with the first load decrease in the middle of the first run. This meant that mark B had to correspond with the end of run one, even though this mark did not coincide with a change in texture in the fracture surface. Consequently, mark C was correlated with the next significant load feature, the end of the second run.

Two marks were observed between mark C and the end of the crack (marks E and F). These were related to the first increase of load to 10kW occurring at the start of the third run, and to the middle of the third run where the rig was shut down. This produced the crack growth curve as indicated by Figure 10.8 and the corresponding log linear curve shown in Figure 10.9. As can be seen, these gave curves of increasing crack depth with time, however the trend was not as smooth as the curves obtained for the earlier gears. The first two points seemed to be inconsistent with earlier results.

*Table 10.3 First Attempt at Crack growth analysis for Gear A2-3*

| Runs | Date | Time (hours) | Load (kW) | Mark Label | Raw Depth (mm) | Crack Depth (mm) |
|---|---|---|---|---|---|---|
| 1 | 20/06/96 | 0 | 0 | A | 37 | 1 |
| 1 | 20/06/96 | 5.2369 | 45 | N | 62 | 1.68 |
| 1 | 21/06/96 | 7.2877 | 45 | B | 115 | 3.12 |
| 2 | 21/06/96 | 11.0136 | 16.3 | C | 134 | 3.62 |
| 3 | 27/06/96 | 11.778 | 10 | D | 149 | 4.03 |
| 3 | 27/06/96 | 14.3064 | 15 | E | 181 | 4.89 |
| 3 | 28/06/96 | 18.5 | 0 | F | 216 | 5.84 |

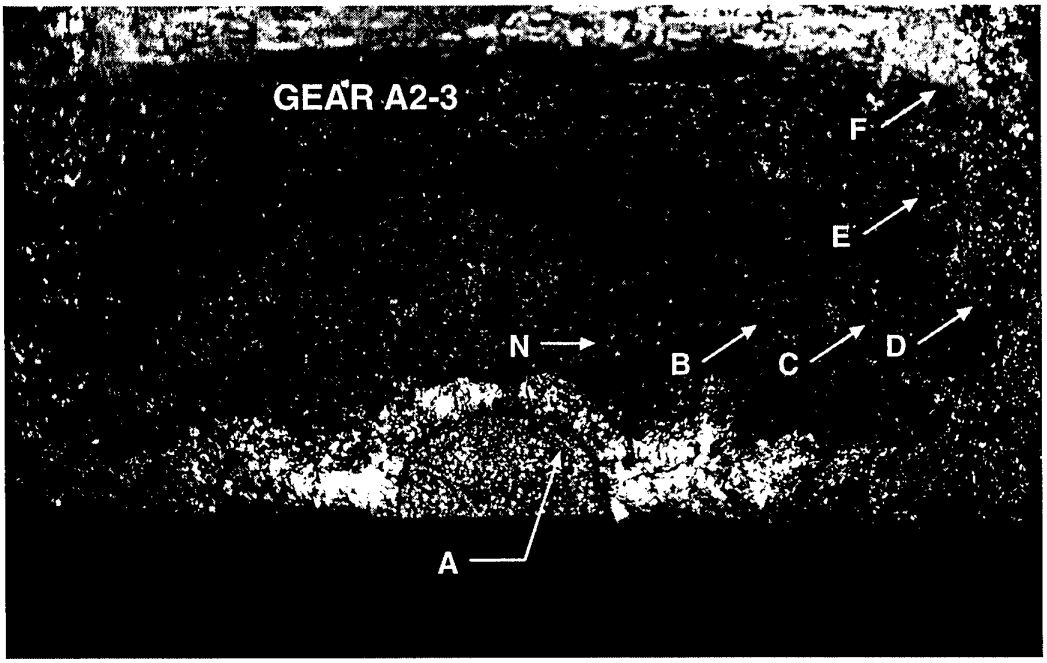


*Figure 10.7 Indication of progression marks on fracture surface of Gear A2-3*

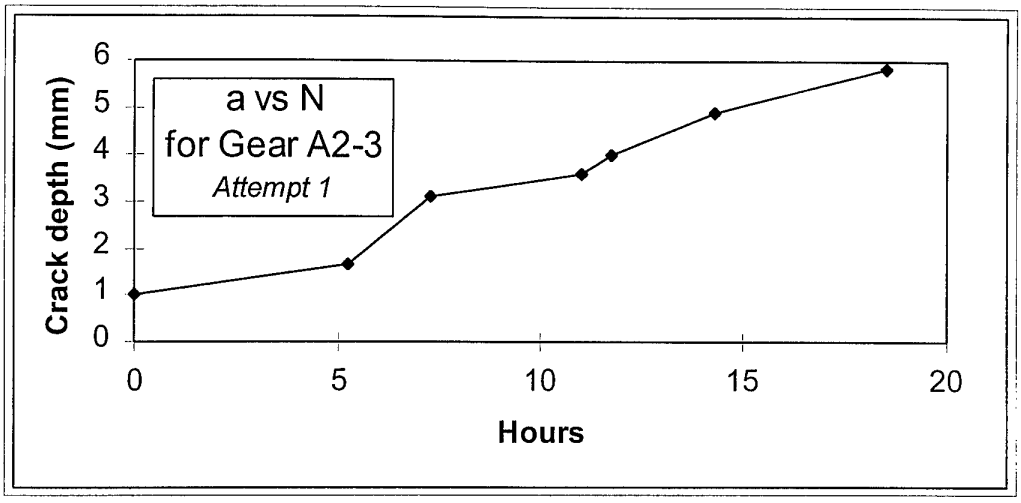


*Figure 10.8 Crack growth curve for Gear A2-3 (First Attempt)*

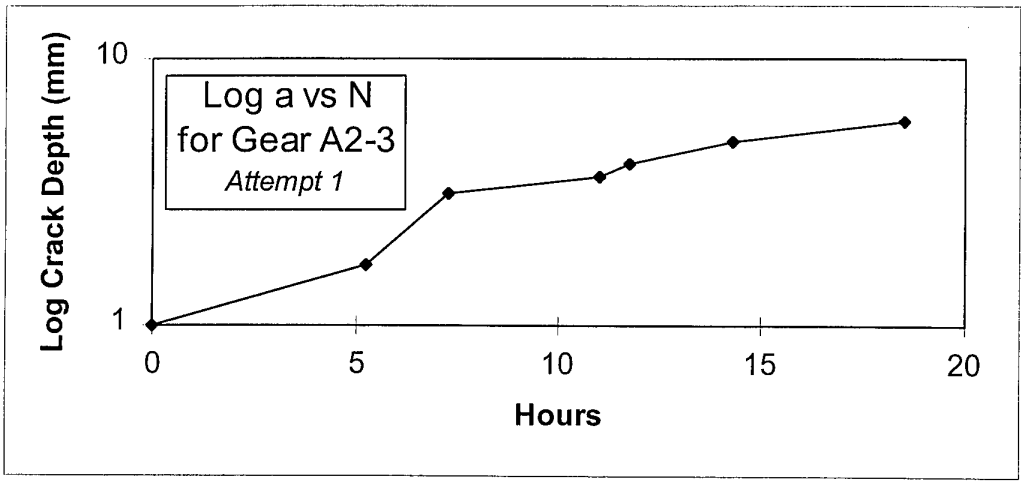


*Figure 10.9 Log Crack growth curve for Gear A2-3 (First Attempt)*

### 10.3.2 Second Attempt

The gear was observed under a binocular microscope, which gave a three dimensional view of the fracture. The lighting used was dark field to give more contrast to the image. This intensified mark N and made it impossible to dismiss it. There were several factors however which when considered, made it illogical for the first mark to relate to the peak in the middle of the first run. These were as follows :

1. Gear A2-1 and Gear A2-2 consistently had the load reaching high values up to 45kW throughout their entire runs. However Gear A2-3 was the only gear so far which had a significant stress change occurring. That is, after the first run being maintained constantly at 45kW, the loads in the second and third runs remained extremely low in comparison. So it was expected that some texture change would occur in that region of the fracture corresponding with that time.

2. The cracks in Gears A2-1 and A2-2 grew to about 2mm in only 3 hours of running at 45kW, so it was expected that Gear A2-3 after 5 hours of running at that same load, would produce a crack depth of at least the same order, particularly since the gear was of the same batch as the previous two gears. Mark N corresponded to a crack depth of only 1.65mm, much less than the expected size of the crack in that time. In addition, the MRI results also indicated that the crack had grown quite extensively, becoming an edge crack at the end of the second run (Figure 8.4).

The only possibility left was the fact that some incident had occurred in the rig during that time which could have caused a mark. This was quite possible since the mark occurs as a result of an interruption to the applied loading. A search of the log file of that particular run, revealed nothing to suggest that any extraordinary event had occurred. The loading remained at 45kW up to 5 hours. However, looking at the kurtosis trend for that run it was noted that a significant drop in the kurtosis had occurred in the middle of the first run. The original log file confirmed that indeed there was a drop in the kurtosis and also the RMS value. Further investigation eventually revealed that the disturbance was due to oil pump modifications (Full details of this are mentioned in Reference 3).

Hence, marks B and C evidently corresponded to the middle and the end of the first run. Mark D which is situated in the newly textured area was correlated with the end of the second run. Finally, mark E, a subtle mark, was correlated with the middle of the third run at the point where the rig was shut down.

The crack growth data for this attempt is shown in Table 10.4. The final crack growth curve for this gear is shown in Figure 10.10. As can be seen the curve is much smoother. There are two distinct sections. The crack starts propagating steeply and then there is a drop in the rate. This was due to the fact that the crack changed direction after becoming an edge crack and the load applied to the gear was significantly reduced. Figure 10.11 shows a similar trend.

*Table 10.4 Crack growth analysis for Gear A2-3 (Second Attempt)*

| Runs | Date | Time (hours) | Load (kW) | Mark Label | Raw Depth (mm) | Crack Depth (mm) |
|---|---|---|---|---|---|---|
| 1 | 20/06/96 | 0 | 0 | A | 37 | 1 |
| 1 | 20/06/96 | 5.2369 | 45 | B | 115 | 3.11 |
| 1 | 21/06/96 | 7.2877 | 45 | C | 134 | 3.62 |
| 2 | 21/06/96 | 11.0136 | 16.3 | D | 149 | 4.03 |
| 3 | 27/06/96 | 11.778 | 10 | | | |
| 3 | 27/06/96 | 14.3064 | 15 | E | 181 | 4.89 |
| 3 | 28/06/96 | 18.5 | 0 | F | 216 | 5.84 |

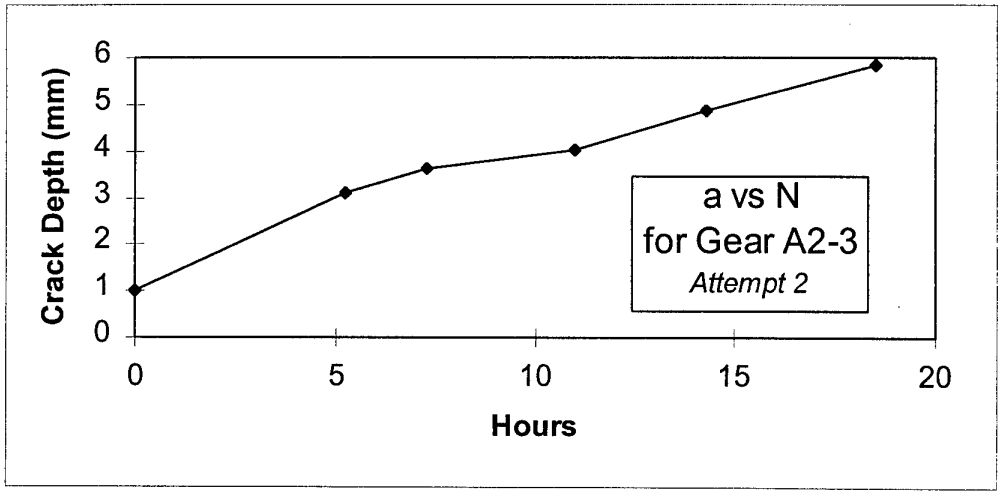


*Figure 10.10 Crack growth curve for Gear A2-3 (Second Attempt)*

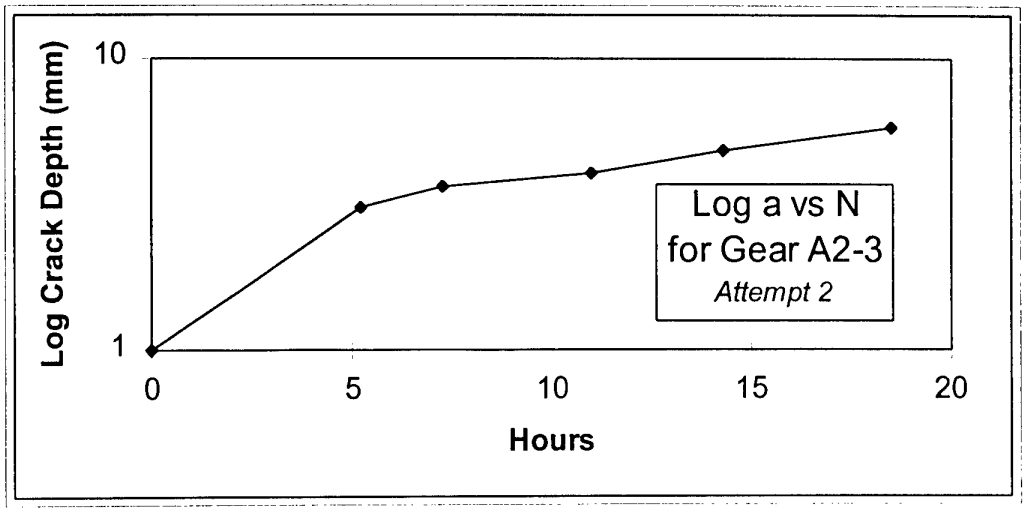


*Figure 10.11 Log-Linear crack growth curve for Gear A2-3 (Second Attempt)*

## 10.4 GEAR A2-5

The values used in the crack curve are shown in Table 10.5 and the fracture surface showing the location of the marks (white arrows) is shown in Figure 10.12. This fracture was stained in many areas making it extremely difficult to find marks. The standard points were obvious in this fracture. That is, the notch as the crack initiation site, and the end of the crack in the overload region. After the notch, there were only two distinct marks which could be observed. From the loading history it was reasonable to assume that these marks would be correlated with the middle and the end of the first run. The first mark occurred in the middle of the stain which made it very difficult to trace the mark along the entire crack front. The second mark could only be observed on one side of the notch but that part of it could be seen very clearly.

The same problem existed as for Gear A2-3, where the load was significantly reduced from 45kW, to low levels in the second and third runs, preventing production of any distinct marks. It was expected that there would be a mark at the end of the second run where the load drop was quite substantial however this placed the mark so close to the end of fracture (since the crack propagated so rapidly) that it was hard to distinguish. The crack growth curve for Gear A2-5 is shown in Figure 10.13. This graph shows the same trend as for Gear A2-3 where it starts off as an exponential curve and then the rate decreases. This behaviour is feasible since the MRI results indicated that the crack grew substantially in the first run but there was only a small amount of propagation thereafter. No real texture change was noticed between the end of the first run and the start of the second, as with the previous gear at that instant. However at that moment, the crack was close to the fast fracture region, so any texture change was hard to see. Figure 10.14 shows the log linear curve for the fracture which shows this change in rate clearly.

*Table 10.5 Crack growth analysis for Gear A2-5*

| Runs | Date | Time (hours) | Load (kW) | Mark Label | Raw Depth (mm) | Crack Depth (mm) |
|---|---|---|---|---|---|---|
| 1 | 9/07/96 | 0.0028 | 0 | A | 37 | 1 |
| 1 | 9/07/96 | 3.9278 | 45 | B | 54 | 1.46 |
| 1 | 10/07/96 | 6.5259 | 45 | C | 84 | 2.27 |
| 3 | 19/07/96 | 12.6 | 0 | D | 91 | 2.46 |

-

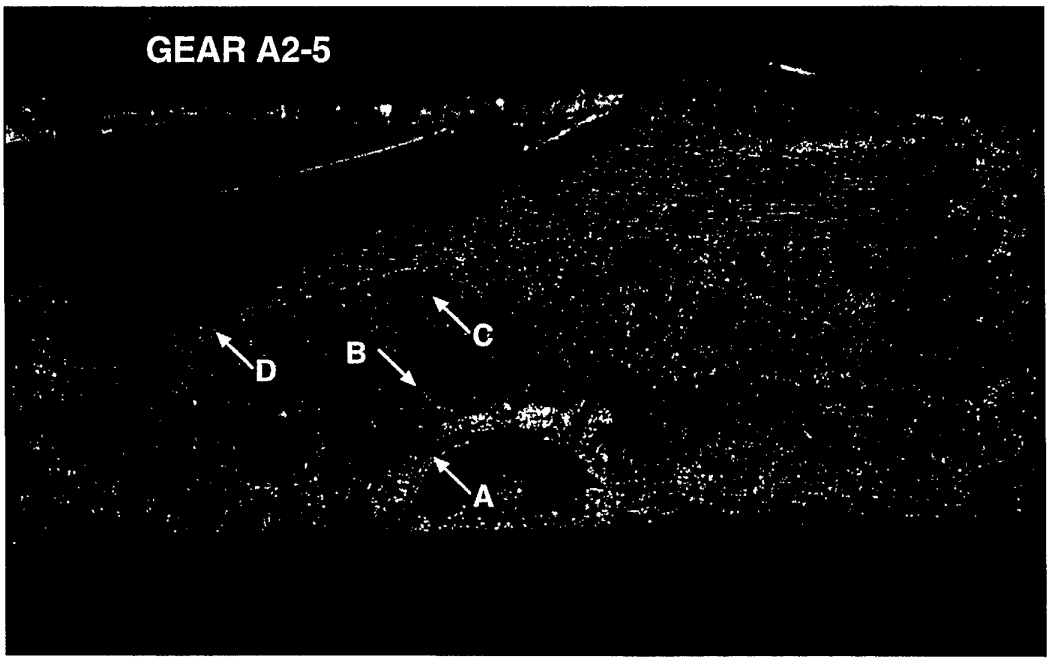


*Figure 10.12 Indication of progression marks on fracture surface of Gear A2-5*

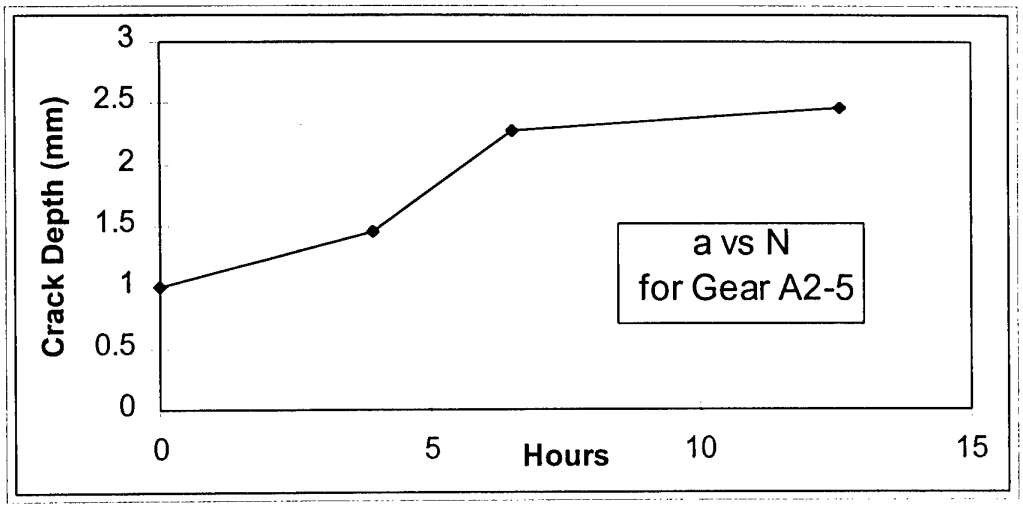


*Figure 10.13 Crack growth curve for Gear A2-5*

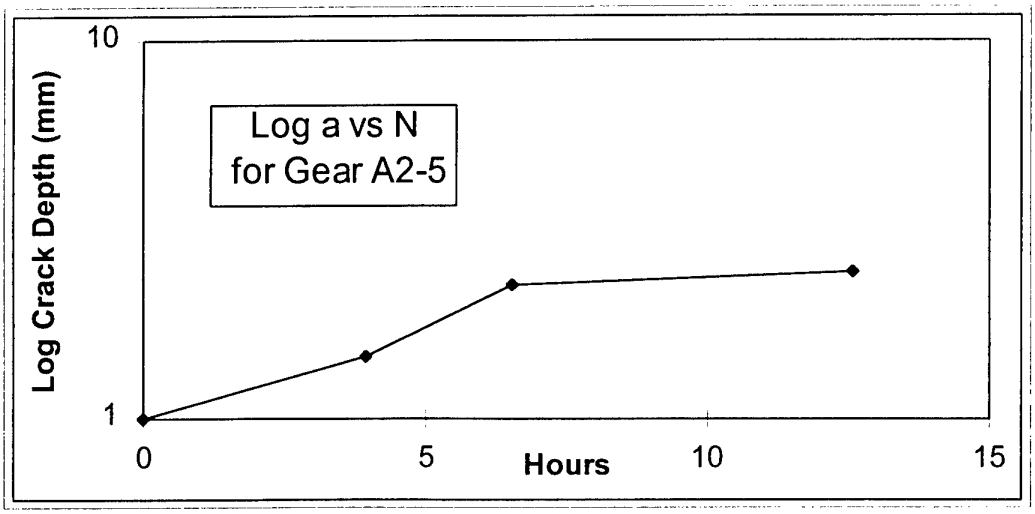


*Figure 10.14 Log-Linear crack growth curve for Gear A2-5*

# 11. Correlation with Kurtosis values

The remaining step was to correlate the crack growth curves obtained from the fractographic measurements with the trend of the kurtosis indices acquired from the gear rig. This had its limitations. The crack growth curves were based on correlating the marks measured on the gear fracture surface, with the applied loading. For most of the gears only a few marks could be seen, due to the characteristics of the surface, or the limited number of load features producing the marks. This resulted in only 4 to 7 points on the crack growth curves. Obviously this provided only a broad indication of what was actually happening in the initial stages of the crack and throughout its life.

In addition it was very difficult to make a direct comparison between the two parameters since one of them was the trend of a physical distance, and the other was the trend of a local condition index obtained from vibration analysis. However if the kurtosis does give an accurate representation of the local condition of the cracked gear tooth, then it is expected that both curves should exhibit the same sort of behaviour.

Figures 11.1 to 11.4 show the trend of the kurtosis superimposed onto the crack growth curves obtained for the four gears. As can be seen, the kurtosis does not have that exponential increase that the crack growth exhibits. Interpretation of the two curves is difficult because the values fluctuate with the termination of runs. Based on these curves however, it is evident that the kurtosis can provide an indication of the presence of the crack, but gives no clear correlation with the progression of the crack over each stage of its life. Therefore it does not appear to be a good indicator of the actual crack growth characteristics of the gear.

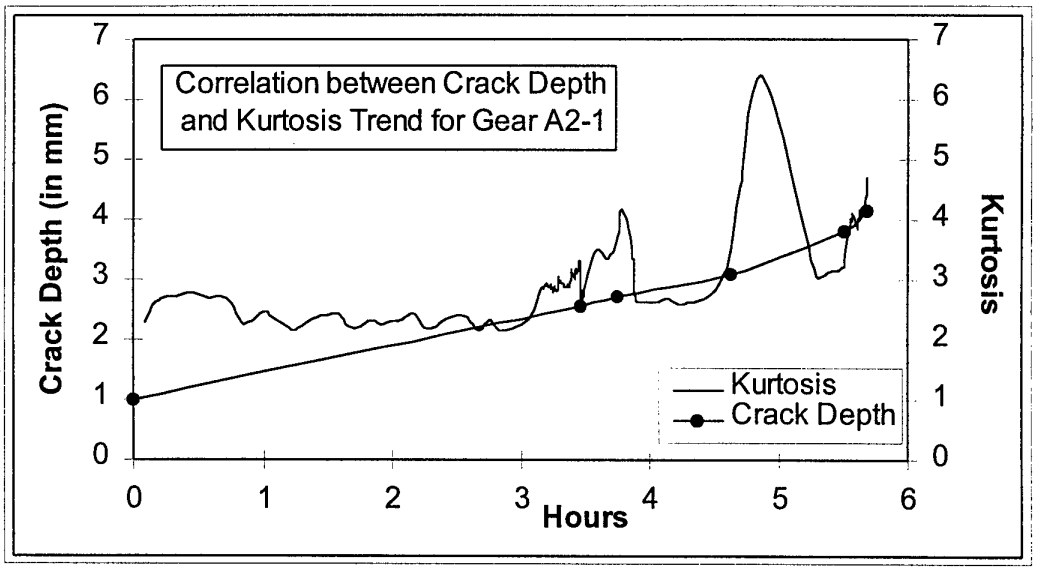


*Figure 11.1 Kurtosis trend of Gear A2-1*

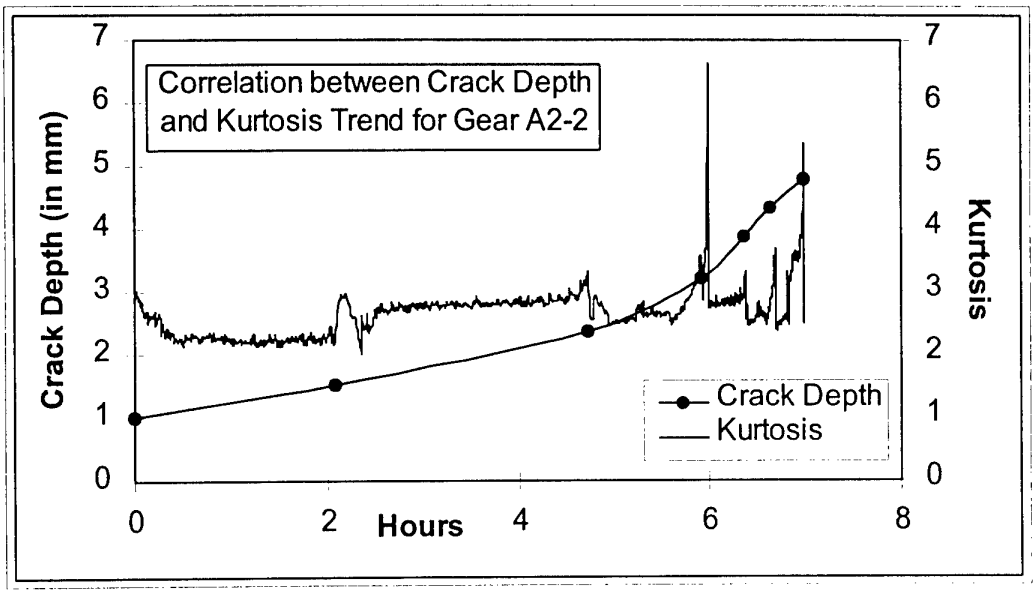


*Figure 11.2 Kurtosis trend of Gear A2-2*

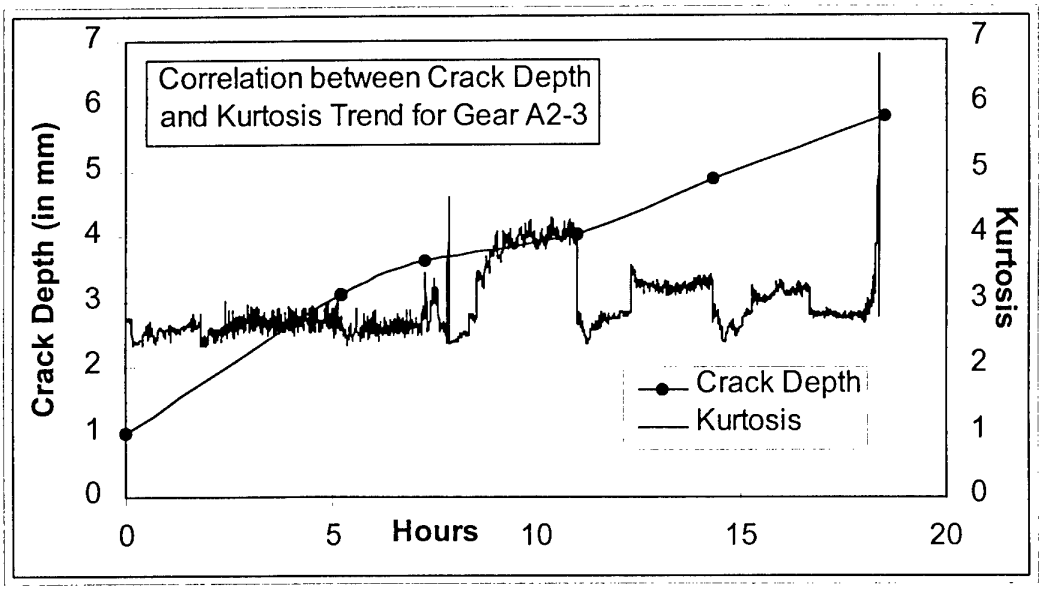


*Figure 11.3 Kurtosis trend of Gear A2-3*

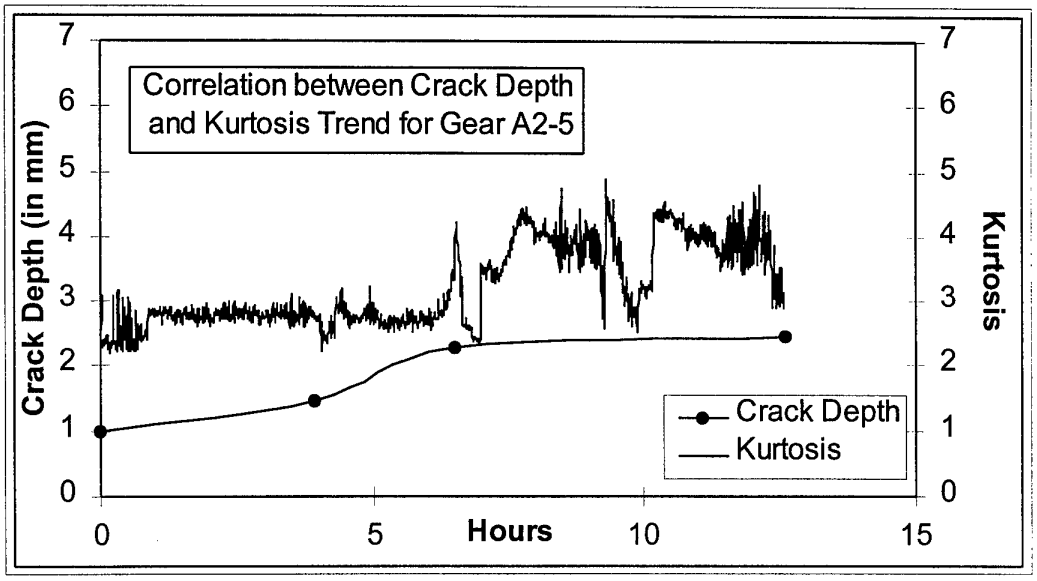


*Figure 11.4 Kurtosis trend of Gear A2-5*

# 12. Discussion and Concluding Remarks

Crack growth curves were obtained for four low-alloy steel spur gears using fractographic methods. Many parameters had to be considered when analysing the fracture surfaces. The quality of illumination was found to be extremely critical to the final results since it determined which marks could or could not be seen. In fact the whole investigation was based on using the best possible methods to locate progression marks and to distinguish them from other marks. In addition, these marks had to be correlated with the load features that caused them. As discussed in Section 10, this was a difficult task and one that required patience and persistence.

There were many factors contributing to the difficulty of locating marks on the fracture surface. There was a large amount of relief on the fracture and a compromise had to be made balancing the depth of field while still obtaining good resolution. As a result, when trying to trace a crack along the whole crack front, the image would continuously go in and out of focus making it easy to lose the location of the mark.

When cracks occur on different planes, they will at some stage overlap. At that instant the behaviour is analogous to a spring. The load is shared and hence the crack growth rate locally is reduced. The result is a fragmented crack front. Consequently the mark will not have a consistent appearance along the crack front. It is quite possible that one mark will change from black to white or undergo a change in texture because of the material characteristics. These factors had to be considered to avoid the danger of looking for only one type of mark.

In some fractures, the peaks in the load history in the later runs, although not as significant as the earlier load peaks, produced distinct marks on the surface. As the crack depth increases, the stress intensity factor K, also increases, and consequently, features in the load occurring at a later stage produce marks that are more pronounced.

Many factors can influence the crack growth curves. The final curves all showed the trend of crack depth increasing with time. Gear A2-1 and Gear A2-2 showed a smooth exponential curve, whereas Gear A2-3 and Gear A2-5 both showed an initial rapid crack propagation followed by a slower propagation rate. This was attributed to the crack reaching the end of the tooth root becoming an edge crack, and also due to the significant change in loading applied to the gears. It is apparent that the loading history has a major influence to what is finally produced in the curves. In these experiments the kurtosis was the governing parameter determining the loading applied to the gear. However this approach leads to complex crack growth behaviour and this does not necessarily produce the desired marks on the fracture surface. Hence, in order to produce curves like those observed for the first two gears, the loading would need to be implemented in such a way as to produce many macroscopic marks along the entire fracture surface, especially near the notch in the initiation stage. One possibility involves running the rig for only one hour at a time at a load of 45kW followed by a sharp drop in load. This would produce the marks required and prevent the crack progressing too rapidly.

Two other parameters were discussed in this investigation. The kurtosis, which is a local fault index obtained from vibration analysis software, and the MRI results. The final values of the MRI results were compared with the final surface crack depths and the final fracture crack depths. In all cases these were found to be in good agreement. However the MRI technique was shown to be limited since it only gave values of crack length initially, until the crack reached the edge where the true crack depth values were obtained. Since the crack depth values usually consisted of one or two points, this was not sufficient to provide a useful comparison with the crack growth curves or kurtosis trends already obtained. The usefulness of the MRI technique lies in two areas. Firstly in conjunction with the gear rig as an indication of the presence and approximate location of the crack. Secondly in connection with the fracture analysis of the gears, as a guide to where any macroscopic progression marks might be located.

Finally, the crack growth curves were plotted together with the kurtosis trends, and an attempt was made to compare and correlate the two curves. More cases will need to be analysed before any final conclusions can be reached, but so far, the graphs do not seem to indicate any correlation. The kurtosis is adequate for the gear rig in terms of indicating the presence of a crack, but does not appear to correlate in any obvious way with the development of the crack from initiation until fracture.

# 13. Acknowledgements

The author wishes to thank :

Noel Goldsmith, for his invaluable assistance and advice with analysing the fracture surfaces of the gears, Nick Athiniotis and Rohan Byrnes, for their assistance and guidance in image analysis and computing support, and Ken Vaughan, for assistance with the Magnetic Rubber Inspection.

# 14. References

1. SHANYAVSKY, A.A AND KUNAVIN, S.A *Mechanism and Diagram Of Individual Fatigue Crack Growth In Aluminium Alloys,* Russian Metallurgy, Metally, No 2, 1984

2. CALLISTER, W.D.Jr, *Materials Science and Engineering - An Introduction,* Second Edition, Wiley, 1991

3. KRAKE, L., *Fault Propagation in a Spur Gear,* AMRL Report (Draft)

4. TURK, S., *Investigation of Striation Spacing in Fatigue Fractures of 7050-T7451 Aluminium Alloy,* DSTO, Vacation Scholar Report, February, 1997

DISTRIBUTION LIST

Crack Growth Behaviour of Spur Gears: A Fractographic Analysis

C. Vavlitis

**AUSTRALIA**

**DEFENCE ORGANISATION**

**Task Sponsor** Director of Technical Airworthiness-Logistics Systems Agency

**S&T Program**

Chief Defence Scientist
FAS Science Policy
AS Science Corporate Management
} shared copy

Director General Science Policy Development
Counsellor Defence Science, London (Doc Data Sheet )
Counsellor Defence Science, Washington (Doc Data Sheet )
Scientific Adviser to MRDC Thailand (Doc Data Sheet )
Director General Scientific Advisers and Trials/Scientific Adviser Policy and Command (shared copy)
Navy Scientific Adviser (Doc Data Sheet and distribution list only)
Scientific Adviser - Army (Doc Data Sheet and distribution list only)
Air Force Scientific Adviser
Director Trials

**Aeronautical and Maritime Research Laboratory**

Director
Chief of Airframes and Engines Division
Research Leader Aerospace Composite Structures (A. Baker)
Research Leader Propulsion (S. Fisher)
Head Fatigue and Fracture Detection and Assessment (G. Clark)
Task Manager (N. Goldsmith)
C. Vavlitis
N. Athiniotis
A. Wong
D. Forrester
B. Rebbechi
D. Blunt
M. Burchill
M. Shilo

**DSTO Library**

Library Fishermens Bend
Library Maribyrnong
Library Salisbury (2 copies)
Australian Archives
Library, MOD, Pyrmont (Doc Data sheet only)

**Capability Development Division**

Director General Maritime Development (Doc Data Sheet only)
Director General Land Development (Doc Data Sheet only)
Director General C3I Development (Doc Data Sheet only)

**Navy**

Senior Propulsion Engineer, Naval Aircraft Logistics Office, Locked Bag 12, Naval Support Command, Pyrmont NSW 2009

**Army**

ABCA Office, G-1-34, Russell Offices, Canberra (4 copies)
SO (Science), DJFHQ(L), MILPO Enoggera, Queensland 4051 (Doc Data Sheet only)
NAPOC QWG Engineer NBCD c/- DENGRS-A, HQ Engineer Centre Liverpool Military Area, NSW 2174 (Doc Data Sheet only)OC, 5 Aviation Regiment Workshop, RAAF Base Townsville, Townsville QLD 4810
A25 Logistics Engineer, Army Aircraft Logistics Management Squadron, Army Airfield, Oakey QLD 4401

**Air Force**

Director of Technical Airworthiness-Logistics Systems Agency, Headquarters Logistic Command
Tech Reports, CO Engineering Squadron, Aircraft Research and Development Unit, RAAF Base Edinburgh SA 5111

**Intelligence Program**

DGSTA Defence Intelligence Organisation

**Corporate Support Program (libraries)**

OIC TRS, Defence Regional Library, Canberra
Officer in Charge, Document Exchange Centre (DEC), 1 copy
*US Defence Technical Information Center, 2 copies
*UK Defence Research Information Centre, 2 copies
*Canada Defence Scientific Information Service, 1 copy
*NZ Defence Information Centre, 1 copy
National Library of Australia, 1 copy

**UNIVERSITIES AND COLLEGES**

Australian Defence Force Academy
Library
Head of Aerospace and Mechanical Engineering
Senior Librarian, Hargrave Library, Monash University
Librarian, Flinders University
Dr I.M. Howard, Department of Mechanical Engineering, Curtin University of Technology, GPO Box U 1987, Perth WA 6001
Prof. R.B. Randall, School of Mechanical and Manufacturing Engineering, University of New South Wales, Sydney NSW 2052
Prof. E. Hahn, School of Mechanical and Manufacturing Engineering, University of New South Wales, Sydney NSW 2052

Dr Y. Gao, School of Mechanical and Manufacturing Engineering, University of New South Wales, Sydney NSW 2052
Mr D. Ho, School of Mechanical and Manufacturing Engineering, University of New South Wales, Sydney NSW 2052
Prof. J. Mathew, Centre for Machine Condition Monitoring, Monash University

**OTHER ORGANISATIONS**
NASA (Canberra)
AGPS

**OUTSIDE AUSTRALIA**

**ABSTRACTING AND INFORMATION ORGANISATIONS**
INSPEC: Acquisitions Section Institution of Electrical Engineers
Library, Chemical Abstracts Reference Service
Engineering Societies Library, US
Materials Information, Cambridge Scientific Abstracts, US
Documents Librarian, The Center for Research Libraries, US

**INFORMATION EXCHANGE AGREEMENT PARTNERS**
Acquisitions Unit, Science Reference and Information Service, UK
Library - Exchange Desk, National Institute of Standards and Technology, US

**THE TECHNICAL CO-OPERATION PROGRAM:**
(Aerospace Systems Group
Technical Panel AER-TP-7,
Propulsive and Mechanical Systems Condition Monitoring and Diagnostics)

**Canada**
Mr. Jeff Bird, Structures, Materials and Propulsion Laboratory, National Research Council Canada Institute for Aerospace Research, Bldg M-7, Montreal Rd, Ottawa, Ontario K1A 0R6, Canada
Mr. Don Rudnitski, Structures, Materials and Propulsion Laboratory, National Research Council Canada Institute for Aerospace Research, Bldg M-7, Montreal Rd, Ottawa, Ontario K1A 0R6, Canada

**United Kingdom**
Mr. Fred Tufnell, FS(Air)42, Ministry of Defence (PE), Maple 0a, MOD Abbey Wood #45, PO Box 702, Bristol BS12 7DU, UK

**United States**
Mr Andrew J. Hess, AIR-4.4.2, Naval Air Warfare Center - Aircraft Division (NAWCAD), Propulsion and Power Bldg #106 Unit 4, 22195 Elmer Rd, Patuxent River, MD 20670-1534, USA

**DEFENCE ORGANISATION:**

**UK Ministry Of Defence**
Mr. J. Nurse, AD/FS(AIR)4, Ministry of Defence(PE), Abbey Wood Maple 0a #45, PO Box 702, Bristol BS12 7DU, UK

**US Air Force**

Mr James Ramsey, USAF - Kirtland Air Force Base, 542 LOGGSS/AFETS, 4150 Hanger Road, Room 102, Kirtland AFB, New Mexico 87117-5000 USA

**US Navy**

Mr Bob Thompson, HSL-1 NAESU, Naval Air Station, North Island, California 92123 USA

**US Army**

Mr. J.F. Tansey, US Army AMSAT-R-TL, AATD, Fort Eustis, Virginia 23604-5577, USA

**NASA**

Mr J.J. Coy, Mechanical Systems Technology Branch, Mail Stop 77-10, NASA Lewis, 21000 Brook Park Road, Cleveland, Ohio 44135 USA

**OTHER ORGANISATIONS**

Mr L.L. Dobrin, Chadwick-Helmuth Company, Inc., 4601 N. Arden Drive, El Monte, California 91731 USA

SPARES (10 copies)

**Total number of copies:** **83**

**DEFENCE SCIENCE AND TECHNOLOGY ORGANISATION**
**DOCUMENT CONTROL DATA**

1. PRIVACY MARKING/CAVEAT (OF DOCUMENT)

2. TITLE

Crack Growth Behaviour of Spur Gears: A Fractographic Analysis

3. SECURITY CLASSIFICATION (FOR UNCLASSIFIED REPORTS THAT ARE LIMITED RELEASE USE (L) NEXT TO DOCUMENT CLASSIFICATION)

| | |
|---|---|
| Document | (U) |
| Title | (U) |
| Abstract | (U) |

4. AUTHOR(S)

C. Vavlitis

5. CORPORATE AUTHOR

Aeronautical and Maritime Research Laboratory
PO Box 4331
Melbourne Vic 3001 Australia

| 6a. DSTO NUMBER | 6b. AR NUMBER | 6c. TYPE OF REPORT | 7. DOCUMENT DATE |
|---|---|---|---|
| DSTO-TN-0137 | AR-010-463 | Technical Note | January 1998 |

| 8. FILE NUMBER | 9. TASK NUMBER | 10. TASK SPONSOR | 11. NO. OF PAGES | 12. NO. OF REFERENCES |
|---|---|---|---|---|
| M1/9/351 | AIR 95/088 | DTA-LSA | 34 | 4 |

13. DOWNGRADING/DELIMITING INSTRUCTIONS

None

14. RELEASE AUTHORITY

Chief, Airframes and Engines Division

15. SECONDARY RELEASE STATEMENT OF THIS DOCUMENT

*Approved for public release*

OVERSEAS ENQUIRIES OUTSIDE STATED LIMITATIONS SHOULD BE REFERRED THROUGH DOCUMENT EXCHANGE CENTRE, DIS NETWORK OFFICE, DEPT OF DEFENCE, CAMPBELL PARK OFFICES, CANBERRA ACT 2600

16. DELIBERATE ANNOUNCEMENT

No Limitations

17. CASUAL ANNOUNCEMENT Yes

18. DEFTEST DESCRIPTORS

Spur Gears, Cracking, Fractography, Vibration Analysis, Kurtosis

19. ABSTRACT

Vibration Analysis offers a means of detecting faults in gear systems without the need for costly periodic overhaul and inspection, and promises substantial cost savings in several military platform applications. The correlation of vibration analyses with fatigue crack growth forms an essential part of ongoing research aimed at maximising the information which can be obtained from vibration analyses. This report discusses the use of fractographic analysis to determine the growth behaviour of fatigue cracks in four case-hardened low-alloy steel spur gears.

TECHNICAL NOTE DSTO-TN-0137 AR-010-463 JANUARY 1998

DSTO AUSTRALIA

AERONAUTICAL AND MARITIME RESEARCH LABORATORY
PO BOX 4331 MELBOURNE VICTORIA 3001
AUSTRALIA, TELEPHONE (03) 9626 7000